The Astrophysical Journal, 763:30 (17pp), 2013 January 20 doi:10.1088/0004-637X/763/1/30

THE "TWIN-CME" SCENARIO AND LARGE SOLAR ENERGETIC PARTICLE EVENTS IN SOLAR CYCLE 23

Liuguan Ding[1,2], Yong Jiang[1], Lulu Zhao[2], and Gang Li[2]
[1] College of Math & Physics, Nanjing University of Information Science & Technology, Nanjing, Jiangsu 210044, China
[2] Department of Physics and CSPAR, University of Alabama in Huntsville, AL 35899, USA; gang.li@uah.edu
Received 2012 August 23; accepted 2012 October 31; published 2013 January 2

ABSTRACT

Energetic particles in large solar energetic particle (SEP) events are a major concern for space weather. Recently, Li et al. proposed a "twin-CME" scenario for ground-level events. Here we extend that study to large SEP events in solar cycle 23. Depending on whether preceding coronal mass ejections (CMEs) within 9 hr exist and whether ions >10 MeV nucleon^{-1} exceed 10 pfu, we categorize fast CMEs with speed >900 km s^{-1} and width >60° from the western hemisphere source regions into four groups: groups I and II are "twin" and single CMEs that lead to large SEPs; groups III and IV are "twin" and single CMEs that do not lead to large SEPs. The major findings of this paper are: *first*, large SEP events tend to be "twin-CME" events. Of 59 western large SEP events in solar cycle 23, 43 are "twin-CME" (group I) events and 16 are single-CME (group II) events. *Second*, not all "twin CMEs" produced large SEPs: 28 twin CMEs did not produce large SEPs (group III events). Some of them produced excesses of particles up to a few MeV nucleon^{-1}. *Third*, there were 39 single fast CMEs that did not produce SEPs (group IV events). Some of these also showed an excess of particles up to a few MeV nucleon^{-1}. For all four groups of events, we perform statistical analyses on properties such as the angular width, the speed, the existence of accompanying metric type II radio bursts, and the associated flare class for the main CMEs and the preceding CMEs.

Key words: acceleration of particles – Sun: coronal mass ejections (CMEs) – Sun: flares – turbulence

Online-only material: color figures

1. INTRODUCTION

Solar energetic particles (SEPs) are a major concern for space weather. Propagating along interplanetary magnetic field lines from the Sun to the Earth, these high-energy particles can pose an extreme deadly radiation dose to astronauts. In addition, they can affect electronics onboard spacecraft as well as commercial flights over the polar regions, causing severe economic consequences (see, e.g., Siscoe 2000; Lanzerotti 2001; Baker 2004; Martens et al. 2010).

SEPs, sometimes reaching energies ~GeV nucleon^{-1}, are produced at and near the Sun mainly via two processes: solar flares and coronal mass ejections (CMEs). Events where particles are accelerated at flares are historically termed as "impulsive" and those where particles are accelerated by CME-driven shocks as "gradual" (Cane et al. 1986; Reames 1995, 1999). These terms describe the main features of the observed temporal profiles of SEPs at 1 AU for these two processes. Besides the observed temporal profiles, spectra, abundances, and ionization states of energetic particles in these two classes also differ substantially (see, e.g., recent surveys on CME-driven shocks and associated SEP events (Desai et al. 2003, 2004; Ho et al. 2003; Kahler 2005; Klecker et al. 2009), and surveys on ion composition and spectra during SEP events (Tylka et al. 1995, 2005; Cohen et al. 2003, 2007; Mewaldt et al. 2005, 2007).

While large SEP events are almost always associated with fast CMEs, not all fast CMEs lead to SEP events. An earlier study (Kahler 1996) showed that although the maximum energy and the intensity of energetic particles in SEP events are generally correlated with shock speed, the scatter is very large. Using the *IMP 8* observation, Kahler et al. (2000) examined 17 proton events in the energy range of 28 MeV $< E <$ 43 MeV from CMEs having speeds 650 km s^{-1} $< V_{sh} <$ 850 km s^{-1}, and found that the peak intensities in these events vary by four orders of magnitude. Kahler et al. (2000) suggested that the ambient energetic particle intensity can be another deciding factor for the generation of a large SEP event. These seed particles may originate from impulsive flares (Mason et al. 1999, 2000) or from preceding CMEs (Gopalswamy et al. 2004).

Later, in a study of 57 large SEP events that had intensity >10 pfu at >10 MeV between 1996 and 2002, Gopalswamy et al. (2004) found a strong correlation between high particle intensity events and the existence of preceding CMEs (within 24 hr of the primary CME). Gopalswamy et al. (2004) also noted that while the average flare size was larger for high-intensity SEP events, the SEP intensity showed poor correlation with the flare size. Kahler (2005) found that SEP-rich CMEs are brighter and are more likely to be streamer blowouts and to follow co-located CMEs within 12 or 24 hr.

Stimulated by Gopalswamy et al. (2004), Li & Zank (2005) noted that if two CMEs erupt closely in time from the same active region (AR), then it is possible that the preceding CME drives a shock and creates an excess of interplanetary turbulence which significantly enhances the scattering rate of particles at the shock driven by the second CME, leading to a more efficient shock acceleration process. Li & Zank (2005) further estimated the acceleration timescale at the second shock and showed that if the wave (turbulence) intensity downstream of the first shock (which is the upstream of the second shock) is enhanced by a factor of 10, then the maximum particle kinetic energy at the second shock can increase by a factor of 32. Li & Zank (2005) noted that the preceding shock can provide the seed population needed at the second shock through a pre-acceleration process.

Extending the work of Li & Zank (2005), Li et al. (2012a) discussed a "twin-CME" scenario for ground-level events (GLEs) in which two CMEs erupt in sequence during a short period of time (9 hr) from the same AR with a pseudo-streamer-like pre-eruption magnetic field configuration. The preceding CME in this scenario is often narrower and slower and the primary CME is wider and faster. Li et al. (2012a) showed that the

magnetic field configuration in this scenario can lead to reconnection between the closed magnetic field lines that enclose the preceding CME and the open magnetic field lines that drape the main CME. This reconnection may allow the flare material accompanying the first CME to leak out in front of the second shock (see their Figure 1). When the second CME erupts and drives a second shock, one finds both an excess of seed population and an enhanced turbulence level in front of the main shock, leading to very efficient particle acceleration.

A key assumption in Li et al. (2012a) is the presence of a high-level seed population in front of the second shock. Direct observation to validate such an assumption is impossible at present. This is because the inferred acceleration site, which is several $R_\odot$ from the surface of the Sun, is too close to the Sun and no current mission/spacecraft have orbits this close to measure the in situ seed population. The future NASA mission *Solar Probe Plus* will approach to within 8.5 $R_\odot$ of the photosphere of the Sun and would therefore provide some valuable information about the seed population. Although it is difficult to know the level of the seed population, we can obtain some compositional information about the seed population through examining the abundance of tracer elements such as ^{3}He and He^+ (Mason et al. 1999). In many large SEP events, ^{3}He is found to be enhanced. Because the abundance of ^{3}He in the bulk solar wind is very low, Mason et al. (1999, 2005) concluded that the seed particles in large SEP events are suprathermal particles and are ^{3}He-rich. ^{3}He can be effectively and preferentially accelerated to energies $\sim$ MeV nucleon^{-1} at flare sites (Mason et al. 2000, 2002); therefore a ^{3}He-rich seed population could be remnant flare particles from earlier flares. These flares need not be associated with the preceding CME (as in the "twin-CME" scenario) since flares often occur more frequently than CMEs. In fact, if flares can produce the seed population needed, the preceding CME may not be needed to generate a large SEP event. We do note, however, that in the "twin-CME" scenario, the existence of the preceding CME and its driven shock provide a natural site for keeping the seed population close to the Sun. This is because the preceding CME and its driven shock can lead to a more turbulent region than a flare can. It is this enhanced turbulence that helps to "keep" the seed particles close to the second shock.

The above discussion suggests that large SEP events can be very complicated. In this work, using observations of large SEP events and fast CMEs in solar cycle 23, we examine if the "twin-CME" scenario also operates in large SEP events. We focus on the data set of large SEP events and fast CMEs in solar cycle 23 where systematic data coverage by *SOHO*/LASCO exists.

We examine the following three related questions.

1. Are large SEP events associated with "twin CMEs"?
2. Can fast single CMEs (i.e., CMEs without preceding CMEs within 9 hr) lead to large SEPs?
3. Are there "twin CMEs" that do not lead to large SEP events?

Understanding these questions can help us to better understand under what circumstances large SEP events, and in particular those of space weather concern, may likely occur.

Our paper is organized as follows: in Section 2 we discuss the data selection procedure; in Section 3 we present our statistical analyses; and Section 4 contains the discussions and the conclusions.

2. DATA SELECTION AND EVENT IDENTIFICATION

For large SEP events, we use the large proton event list from the NOAA "Solar Proton Events Affecting the Earth Environment" list, which covers the range 1997–2009: http://www.swpc.noaa.gov/ftpdir/indices/SPE.txt. A large proton event is defined with intensity >10 pfu (1 pfu = 1 proton cm^{-2} s^{-1} sr^{-1}) in the >10 MeV channel of the *Geostationary Operational Environmental Satellites (GOES)* instrument.

We identify the main CME from the Coordinated Data Analysis Workshop (CDAW) Data Center CME list. We only consider events where the main CME occurs in the western hemisphere. We do not consider eastern events because the magnetic connection in these events can be poor. A poor connection can affect the peak proton flux, therefore adding another complication to our study. We require that there are noticeable increases of >10 proton flux from *GOES* observation within 24 hr of the onset of the main CME. Besides *GOES* data, we also check various channels from the Solar Isotope Spectrometer (SIS) and Ultra Low Energy Isotope Spectrometer (ULEIS) instruments on board the spacecraft *Advanced Composition Explorer* (*ACE*). Typically, the peak of high-energy particles (e.g., >100 MeV *GOES* proton) occurs within a few hours of the onset of the main CME. For CMEs propagating toward the Earth, the peaks of ions (often at lower energy channels) can occur at the shock passage.

Since we are interested in the differences between CMEs that cause large SEPs and those that do not cause large SEPs, we also examine CMEs with source regions in the western hemisphere that did not lead to large SEPs. Because most CMEs that cause large SEPs have speeds larger than 900 km s^{-1}, we have chosen 900 km s^{-1} as the speed threshold of these non-SEP CMEs.

The flare information is from CDAW and http://www.solarmonitor.org. In verifying this information, we have visually examined the movies from CDAW for these events. We note that because of the limited spatial and time resolution of the *Solar and Heliospheric Observatory* (*SOHO*) mission's Extreme ultraviolet Imaging Telescope (EIT), for periods with multiple flares, the association of a flare with size smaller than *M*1.0 to a particular AR can sometimes be tricky. Note that although CMEs having eastern source regions can lead to large SEP events, the magnetic connection in these events is often poor. Therefore we do not conduct statistical analyses for eastern CMEs.

SEP lists from Gopalswamy et al. (2004) and Cane et al. (2006) are also used in this study. Since the CME data in this study were mainly from the *SOHO* mission's Large Angle and Spectrometric Coronagraph (LASCO) instrument, we excluded events that occurred during the period of temporary disability (1998 June to October and 1999 January, and other short periods of data gap) of *SOHO*.

We have excluded eastern events on 1999 May 3, 2001 November 17, and 2002 January 8 from the list of Gopalswamy et al. (2004). We further excluded the event on 2001 April 26 as there was a ~2 hr *SOHO* data gap shortly after the flare in that event. Because there was the possibility that a flare or another CME occurred in that gap, we do not consider this event in the following. We do note that the 2001 April 26 event would be a "twin-CME" event (see below) even if there was no activity during the gap.

Following Li et al. (2012a), a "twin-CME" event is where a preceding CME occurs within 9 hr of the main CME. In identifying the preceding CMEs, we set a speed threshold of 300 km s^{-1}. In the study of Evans & Opher (2008), the Alfvén wave speed for eight different models was considered. All but

one model (numbered "M7" in Evans & Opher 2008) has values of V_A smaller than 300 km s^{-1} at $\sim$2 $R_\odot$–3 $R_\odot$, suggesting shock generation at this height is possible. The choice of 9 hr within which the preceding CMEs erupt prior to the onset time of the main CME is based on the estimate of the decay time of the turbulence downstream of the preceding CME-driven shock (see Li et al. 2012a). It should be understood as an empirical choice and slight variation of it should not alter the conclusion of this study. Interestingly, we note that in a recent study by Chen et al. (2011), the waiting time of consecutive CMEs from the same AR was examined and found to have two populations, above and below 8 hr, respectively. Below 8 hr, the second one is unlikely to be a fast CME if the first one is. The choice of 9 hr in our study is similar to the 8 hr gap found in Chen et al. (2011). We impose no threshold on the angular width of the preceding CME. However, we do require the centerline of the preceding CME to be within the angular span of the main CME as projected onto the plane of the sky. We note that the projection effect may lead to the largest uncertainties in our analysis.

In identifying the preceding CMEs, we make use of various online catalogs including the CDAW Data Center catalog at http://cdaw.gsfc.nasa.gov/CME_list/, the Solar Eruptive Event Detection System (SEEDS) catalog at http://spaceweather.gmu.edu/seeds/ (Olmedo et al. 2008), and the Computer Aided CME Tracking (CACTus) catalog at http://sidc.oma.be/cactus/. If a CME exists in multiple databases, the CDAW database is given priority. We note that the onset time of a CME in LASCO/C2, the central position angle (CPA), the width, and the CME speed for the same CME may be different in different databases.

Based on these conditions, we classify all CMEs in our study to four groups. Group I are "twin CMEs" that lead to large SEPs; group II are single CMEs that lead to large SEPs; group III are "twin CMEs" that do not lead to large SEPs; and group IV are single CMEs that do not lead to large SEPs.

2.1. Large SEP Events

Table 1 lists 75 western SEP events.

Among these, 16 events have flare longitudes $\geqslant$ western 90°. For these backside events, the determination of preceding flares and CMEs is subject to large uncertainties and we do not consider them in the following statistical analyses. In the remaining 59 events, 43 are "twin-CME" events (i.e., group I events) and 16 are single-CME events (i.e., group II events).

The first column is the event number. The second column is the SEP date. The third column is the onset time of energetic particles as observed from the *GOES* satellite. Columns 4–7 are the CME onset time (its first appearance in LASCO/C2; Gopalswamy et al. 2004), CME center of position angle, CME angular width (WD), and the projection speed (linear fit) on the plane of the sky. For halo CMEs, we use the widths from Cane et al. (2010) or assign 360° to them if they did not appear in Cane et al. (2010). Columns 8 and 9 are the active source region (AR) number and its location. For backside events, we label them by "bs" in Column 8. For the event on 2002 January 14, the EIT movies showed no clear source regions and we label it by "fp" in Column 8. It might be caused by filaments or prominence eruption. Columns 10 and 11 are the flare class and the flare onset time of the flare that is associated with the main CME. These data are obtained from the Solar Geophysical Data database at http://www.solarmonitor.org. We label events where we cannot identify the AR and/or the associated flares by "-" in Columns 10 and 11. The metric type II radio bursts associated with the main CMEs were obtained from the online catalog at http://www.ngdc.noaa.gov/stp/solar/. The start time as observed by the RSTN observatory matrix is listed in Column 12. If no radio bursts were observed, we label it by "n." Column 13 is the onset time of DH type II radio bursts observed by *WIND*/Waves associated with main CMEs from the online catalog at http://cdaw.gsfc.nasa.gov/CME_list/radio/waves_type2.html. Column 14 is the peak flux intensity in the $>$10 MeV nucleon^{-1} channel of the *GOES* satellite of the event. Column 15 is the time interval between the main CMEs and the preceding CMEs. If more than one preceding CME occurred within the threshold, we chose the one having faster speed and/or wider width and/or with clear identification of associated flares. If no preceding CMEs are found we label it by "np." Column 16 of Table 1 is the closest preceding flare found within 9 hr of the main CME.

2.2. The Preceding CMEs for Group I Events

For group I events in Table 1, we list the corresponding preceding CMEs in Table 2. We follow Li et al. (2012a) and set a speed threshold of 300 km s^{-1} in identifying the preceding CMEs.

In Table 2, the first column is the event number; the second column is the SEP date; the third column is the preceding CME's onset time; the fourth column the preceding CME's CPA angle; the fifth column the preceding CME's angular width; and the sixth column the preceding CME's projection speed (linear fit) on the plane of the sky. The classes and onset times of flares associated with the preceding CMEs are listed in Columns 7 and 8. For about half of these preceding CMEs we could not identify associated flares. This is consistent with the fact that preceding CMEs are often not fast nor wide and the associated flares could be very weak. Among all preceding CMEs, only six events were found to have metric type II radio bursts. The onset times of these type II radio bursts are listed in Column 9 (with label "n" denoting no metric type II bursts). Column 10 lists the onset time of DH type II radio bursts observed by *WIND*/Waves. Column 11 lists the database from which the preceding CME is identified.

In Table 1 we have also examined pre-flares (within 9 hr) of a large SEP event. Often, multiple flares within 9 hr of the main CME could be identified. All of these preceding flares and particularly those after the preceding CME can provide the seed population. Note that the presence of the preceding CME may help to keep the pre-accelerated seed particles at the preceding flares close to the main CME-driven shock.

Although events on 2001 April 02 and 2004 April 11 are categorized as "np" events, preceding CMEs 9.3 and 9.6 hr prior to the main CMEs were found for these two events, respectively. Since the uncertainties in deciding the onset times for the preceding CMEs and the main CMEs are roughly the time resolution of *SOHO*/LASCO, which is $\sim$20 minutes, these two events could have been "twin-CME" events. Nevertheless in this study we categorize them as "np" events, i.e., group II events. For another four "np" events—the 2001 March 29, the 2002 April 21, the 2003 October 29, and the 2004 November 10 events—preceding CMEs within 9 hr were identified, but the speeds of the preceding CMEs in these four events were below 300 km s^{-1}. However, these preceding CMEs are identified by the SEEDS catalog only. Olmedo et al. (2008) noted that for the same CMEs, the speeds from the SEEDS catalog are systematically smaller than those obtained from the CDAW catalog (see their Figure 7(c) for a comparison). From our

Table 1
Properties of Large SEP Events and their Associated CMEs, Flares, and Radio Bursts in Solar Cycle 23

Event No. (1)	SEP[a] Date (2)	Time[b] (3)	CME[c] Time (4)	CPA (deg) (5)	WD (deg) (6)	Speed (km s^{-1}) (7)	AR[d] No. (8)	AR Loc. (9)	FC[e] (10)	Flare Onset (11)	Type II[f] (Metric) (12)	Type II (DH) (13)	I_p (pfu) (14)	Δt[g] (hr) (15)	Pre-flare[h] (FC/Δt_1) (16)
1	1997 Nov 4	07:00	06:10	Halo	100	785	8100	S14W33	X2.1	05:52	05:58	6:00	72	np	M4.1/3.6
2	1997 Nov 6	13:00	12:10	Halo	115	1556	8100	S18W63	X9.4	11:49	11:53	12:20	490	7.8	C4.7/0.6
3	1998 May 2	14:00	14:06	Halo	130	938	8210	S15W15	X1.1	13:31	13:41	14:25	150	8.6	C1.4/4.0
4	1998 May 6	08:24	08:29	309	190	1099	8210	S11W65	X2.7	07:58	08:03	08:25	210	8.5	M2.9/1.3
5	1999 Jun 4	08:00	07:26	289	150	2230	8552	N17W69	M3.9	06:52	07:02	07:05	64	6.6	M1.0/0.8
6	2000 Apr 4	17:00	16:32	Halo	60	1188	8933	N16W66	C9.7	15:12	15:25	15:45	55	1.4	-/-
7	2000 Jun 10	18:00	17:08	Halo	120	1108	9026	N22W38	M5.2	16:40	16:55	17:15	46	6.8	C2.6/6.8
8	2000 Jul 14	11:00	10:54	Halo	360	1674	9077	N22W07	X5.7	10:03	10:19	10:30	24000	2.0	C7.1/4.0
9	2000 Jul 22	12:00	11:54	256	229	1230	9085	N14W56	M3.7	11:17	11:25	11:45	17	np	-/-
10	2000 Sep 12	13:00	11:54	Halo	100	1550	9163	S17W09	M1.0	11:31	11:33	12:00	320	3.8	-/-
11	2000 Oct 25	12:00	08:26	Halo	130	770	9199	N10W66	C4.0	08:45	n	09:30	15	4.3	C2.1/2.7
12	2000 Nov 8	23:30	23:06	271	170	1738	9213	N10W77	M7.4	22:42	23:15	23:20	14800	6.0	C6.2/1.4
13	2000 Nov 24	16:00	15:30	Halo	360	1245	9236	N22W07	X2.3	14:51	15:07	15:25	940	3.6	C2.4/3.9
14	2001 Jan 28	17:00	15:54	Halo	120	916	9313	S04W59	M1.5	15:40	n	15:45	49	6.4	-/-
15	2001 Mar 29	11:00	10:26	Halo	360	942	9393	N20W19	X1.7	09:57	10:03	10:12	35	np	C5.5/5.3
16	2001 Apr 2	23:00	22:06	261	244	2505	9393	N18W82	X20	21:32	21:51	22:05	1100	np	M2.1/4.0
17	2001 Apr 10	08:00	05:30	Halo	360	2411	9415	S23W09	X2.3	05:06	05:13	05:24	355	3.4	-/-
18	2001 Apr 12	12:00	10:31	Halo	120	1184	9415	S19W42	X2.0	09:39	10:18	10:20	51	np	M1.3/7.6
19	2001 Apr 15	14:00	14:06	245	167	1199	9415	S20W85	X14	13:19	13:48	14:05	951	2.8	C5.3/3.2
20	2001 Sep 15	12:00	11:54	263	130	478	9608	S21W49	M1.5	11:04	11:29	11:50	11	np	-/-
21	2001 Oct 1	13:00	05:30	Halo	80	1405	9628	S20W84	M9.1	04:41	n	05:36	2360	3.6	-/-
22	2001 Oct 19	17:30	16:50	Halo	160	901	9661	N15W29	X1.6	16:13	16:24	16:45	11	1.7	-/-
23	2001 Nov 4	17:00	16:35	Halo	360	1810	9684	N06W18	X1.0	16:03	16:10	16:30	31700	2.4	-/-
24	2001 Nov 22	21:00	20:30	Halo	360	1443	9698	S24W68	M3.8	20:18	20:22	20:50[j]	10	np	-/-
25	2001 Nov 23	00:00	23:30[i]	Halo	270	1437	9704	S15W34	M9.9	22:32	22:30	22:40	18900	2.0	C5.9/1.5
26	2001 Dec 26	05:30	05:30	281	212	1446	9742	N08W54	M7.1[j]	04:32[j]	05:02	05:20	779	3.4	-/-
27	2002 Jan 14	06:00	05:35	Halo	360	1492	fp	S28W83	M4.4	05:29	06:08	06:25	15	np	-/-
28	2002 Feb 20	06:30	06:30	Halo	50	952	9825	N12W72	M5.1	05:52	06:15	06:20[j]	13	3.0	M4.2/3.8
29	2002 Mar 16	03:00	23:06[i]	Halo	360	957	9866	S08W03	M2.2	22:09	n	22:45	13	np	-/-
30	2002 Mar 18	06:00	02:54	Halo	160	989	9866	S09W46	M1.0	02:16	n	02:55	53	6.8	-/-
31	2002 Apr 17	10:30	08:26	Halo	70	1240	9906	S14W34	M2.6	07:46	08:08	08:30	24	np	-/-
32	2002 Apr 21	02:00	01:27	Halo	120	2393	9906	S14W84	X1.5	00:43	01:19	01:30	2520	np	C1.9/2.1
33	2002 May 22	06:00	03:50	Halo	120	1557	9948	S15W70[k]	C5.0[j]	03:18[j]	n	04:10[j]	820	3.7	-/-
34	2002 Jul 16	10:30	21:30[i]	14	188	1300	10030	N19W01	M1.8	21:03	n	21:15	234	1.0	X3.0/1.5
35	2002 Aug 14	03:00	02:30	297	133	1309	10061	N09W54	M2.3	01:47	01:57	02:20	26	np	-/-
36	2002 Aug 22	02:30	02:06	Halo	80	998	10069	S07W62	M5.4	01:47	01:55	02:45[j]	36	8.6	C3.1/2.1
37	2002 Aug 24	01:30	01:27	Halo	150	1913	10069	S02W81	X3.1	00:49	01:09	01:45	317	4.6	-/
38	2002 Sep 6	04:00	02:06[l]	241	88	737	10095	N08W31	-	-	n	n	208	2.6	-/-
39	2002 Nov 9	15:00	13:31	Halo	90	1838	10180	S12W29	M4.6	13:08	13:17	13:20	404	2.6	C6.3/1.8
40	2003 May 28	04:00	00:50	Halo	360	1366	10365	S07W20	X3.6	00:17	00:26	01:00	121	1.0	X1.3/1.9
41	2003 May 31	02:39	02:30	Halo	150	1835	10365	S07W65	M9.3	02:13	02:20	03:00	27	2.0	-/-
42	2003 Oct 26	18:25	17:54	270	171	1537	10484	N04W43	X1.2	17:21	17:35	17:45	466	np	M1.0/3.6
43	2003 Oct 29	21:00	20:54	Halo	360	2029	10486	S15W02	X10	20:37	20:40	20:55	1570	np	C8.1/4.1
44	2003 Nov 2	11:00	09:30	Halo	120	2036	10486	S17W55	-	-	n	n	30	1.0	M1.0/2.5
45	2003 Nov 2	18:00	17:30	Halo	130	2598	10486	S14W56	X8.3	17:03	17:14	17:30	1570	8.0	-/-
46	2003 Nov 4	22:25	19:54	Halo	130	2657	10486	S19W83	X17	19:29	19:42	20:00	353	7.8	M1.1/6.2
47	2003 Nov 20	08:30	08:06	Halo	360	669	10501	N01W08	M9.6	07:35	n	n	13	5.3	C3.8/0.7
48	2003 Dec 2	12:30	10:50	261	150	1393	10508	S19W89	C7.2	09:39	n	11:00	86	5.0	C3.9/2.9
49	2004 Apr 11	06:00	04:30	203	314	1645	10588	S16W46	C9.6	03:54	n	04:20	35	np	-/-
50	2004 Jul 25	18:55	14:54	Halo	130	1333	10652	N08W33	M1.1	14:19	n	15:00	2086	1.4	M2.2/1.3
51	2004 Nov 7	18:00	16:54	Halo	150	1759	10696	N09W17	X2.0	15:42	15:59	16:25	495	7.0	C2.3/1.7
52	2004 Nov 10	03:00	02:26	Halo	120	3387	10696	N09W49	X2.5	01:59	02:07	02:25	300	np	-/-
53	2005 Jan 16	00:10	23:06[i]	Halo	360	2861	10720	N15W05	X2.6	22:25	22:34	23:00	365	8.2	M1.0/1.1
54	2005 Jan 17	13:05	09:54	Halo	360	2547	10720	N15W25	X3.8	09:41	09:43	09:43	5040	0.4	X2.2/0.8
55	2005 Jan 20	07:00	06:54	Halo	80	882	10720	N14W61	X7.1	06:36	06:44	07:15	1680	2.8	C4.8/3.6
56	2005 Jul 13	17:00	14:30	Halo	70	1423	10786	N08W79	M5.0	14:01	n	14:15	13	1.6	M3.2/2.4
57	2005 Aug 22	19:30	17:30	Halo	100	2378	10798	S12W60	M5.6	16:46	n	17:15	330	3.2	-/-
58	2006 Dec 13	03:10	02:54	Halo	180	1774	10930	S06W23	X3.4	02:14	02:26	02:45	698	6.4	-/-
59	2006 Dec 14	22:55	22:30	Halo	70	1042	10930	S06W46	X1.5	21:07	22:09	22:30	215	2.0	C1.2/5.9
60	1998 Apr 20	11:00	10:07	284	165	1863	8194	S43W90	M1.4[j]	09:38[j]	09:56	10:25	1700	6.8	-/-
61	1998 May 9	05:00	03:35	262	178	2331	8210	S11W90	M7.7	03:04	03:26	03:35	12	1.0	M3.1/1.8
62	1999 Apr 24	15:00	13:31	Halo	120	1495	bs	>NW90	-	-	n	13:50[j]	32	2.4	-/-
63	1999 Jun 1	20:00	19:37	Halo	180	1772	bs	>NW90	-	-	n	18:50	48	6.2	-/-
64	2000 Feb 18	10:00	09:54	286	118	890	bs	>NW90	-	-	09:19	09:38[j]	13	1.0	-/-

Table 1
(Continued)

Event No. (1)	SEP[a] Date (2)	Time[b] (3)	CME[c] Time (4)	CPA (deg) (5)	WD (deg) (6)	Speed (km s^{-1}) (7)	AR[d] No. (8)	AR Loc. (9)	FC[e] (10)	Flare Onset (11)	Type II[f] (Metric) (12)	Type II (DH) (13)	I_p (pfu) (14)	Δt[g] (hr) (15)	Pre-flare[h] (FC/Δt_1) (16)
65	2000 Jul 28	01:30	19:54[i]	Halo	360	905	bs	>NW90	-	-	n	n	18	np	-/-
66	2000 Oct 16	08:00	07:27	Halo	90	1336	9193	N04W90	M2.5	06:40	07:08[j]	07:10	15	1.0	C7.0/1.9
67	2001 Apr 18	03:00	02:30	Halo	140	2465	9424	S23W92[j]	C2.2	02:11	02:17	02:55	321	7.6	-/-
68	2001 May 7	13:00	12:06	286	205	1223	bs	>NW90	-	-	n	13:12[j]	30	2.0	-/-
69	2001 Jun 15	16:00	15:56	Halo	130	1701	bs	>SW90	-	-	15:33	15:42[j]	26	8.4	-/-
70	2001 Aug 16	01:00	23:54[i]	Halo	180	1575	bs	>SW90	-	-	23:31	00:10[j]	493	np	-/-
71	2002 Mar 22	13:30	12:30	243	120	875	9866	S09W90	M1.6	10:12	n	13:10	16	1.4	M1.6/2.3
72	2002 Jul 7	13:00	11:30	277	228	1423	10017	S13W90	M1.0	11:15	n	11:35	22	7.4	-/-
73	2004 Nov 1	06:55	06:06	266	146	925	10687	>W90	-	-	n	05:55	63	2.2	C2.6/1.9
74	2005 Jul 14	13:00	10:54	Halo	360	2115	10786	N11W90	X1.2	10:16	n	11:00	134	3.0	M9.1/4.9
75	2005 Jul 17	13:30	11:30	Halo	120	1527	bs	>NW90	-	-	n	11:50	20	1.6	-/-

Notes.
[a] Date of SEP events.
[b] Onset time of SEP events, following Gopalswamy et al. (2004).
[c] First appearance time of associated CME in LASCO/C2, following Gopalswamy et al. (2004).
[d] Source active region: "bs" denotes backside event and "fp" denotes no NOAA active region number and possibly a filament/prominence eruption.
[e] Onset time of associated flare: "-" denotes that no flares are identified.
[f] Onset time of associated metric type II radio bursts: "n" denotes that no bursts were observed.
[g] The time intervals between the main CME and the preceding CME. "np" denotes that no preceding CMEs within 9 hr were found.
[h] The closest preceding flare found within 9 hr of the main CME. Δt_1 is the time interval between the main CME and the preceding flare.
[i] This time corresponds to the previous day.
[j] From Gopalswamy et al. (2004).
[k] From Shen et al. (2006); this CME triggers a nearby filament eruption, which caused a second enhancement of the energetic particle fluxes.
[l] This CME is detected only by the SEEDS database.

study, we also find that for CMEs that are identified by multiple catalogs (CDAW, SEEDS, and CACTus), the SEEDS catalog often yields the smallest CME speeds (and smallest CME widths) by about 20%. Therefore these four preceding CMEs could potentially be "twin-CME" events as well. Until further re-examinations, however, in this study we still categorize these four events as group II, "np" events.

For the 2005 January 17 event, a preceding CME within 0.5 hr was identified. Careful examination of the *SOHO*/LASCO data confirmed that this preceding CME was indeed an independent CME, not merely an early phase of the main CME.

2.3. "Twin CMEs" with no Large SEPs

We now examine "twin CMEs" that do not lead to large SEP events. From Table 1, we see that all events have CME widths larger than 60°. Therefore, to best compare with the CMEs in Table 1, we focus on CMEs having angular width >60°. In an early study, Kahler & Reames (2003) noted that no fast (v > 900 km s^{-1}) CMEs with angular widths W < 60° were associated with SEP events.

We select the main CMEs from the CDAW database using the following criteria: (1) the speed is faster than 900 km s^{-1}, (2) the angular width is larger than 60°, and (3) the source location is on the western hemisphere with a longitude smaller than 90°.

Table 3 (main CMEs) and Table 4 (preceding CMEs) show 30 "twin CMEs" that we identified in solar cycle 23 which did not lead to large SEP events.

In Table 3, Column 1 is the event number, Column 2 is the event date, and Column 3 is the CME onset time. Columns 4–6 are the CPA, WD, and speed of the CMEs, respectively. Columns 7 and 8 are the active source region (AR) number and its location. Columns 9 and 10 are the flare class and the flare onset time. Columns 11 and 12 are the onset times of the metric and DH type II radio bursts, respectively. Column 13 is the time difference between the main CME and the preceding CME. Column 14 contains comments. Column 15 (the last column) is the closest preceding flares.

In Table 4, Column 1 is the event number, Column 2 is the event date, and Column 3 is the preceding CME onset time. Columns 4–6 are the CPA, WD, and speed of the preceding CMEs, respectively. Columns 7 and 8 are the flare class and the flare onset time. Columns 9 and 10 are the onset time of the metric and DH type II radio bursts, respectively. Column 11 is the database (CDAW, SEEDS, and CACTus) from which the preceding CME is identified.

The 2000 June 17 event and the 2002 October 25 event (labeled by "x" in Column 14 of Table 3) had insufficient EIT information to deduce the source regions of the main and/or the preceding CMEs. It is therefore unclear if these two events were true "twin-CME" events. We do not consider these two events in the following.

For the remaining 28 events, the three events on 2000 November 24, 2001 April 5, and 2003 November 3 all had background of the >10 MeV channel exceeding 10 pfu, but they showed no enhancements from the background. These events are labeled by "hb" in Column 14 in Table 3. For the remaining 25 events, we have examined the low-energy channels of ULEIS and high-energy channels of SIS on *ACE* and found that 18 events showed some enhancement at the ULEIS energy channels and 15 of these 18 events showed weak enhancement at the SIS energy channels (compared to pre-event intensities). In 10 of these 18 events preceding flares also existed. These events are labeled by "e" in Column 14 in Table 3. In some of these events, such as the 2001 April 26 event and the 2003 March 18 event, the main CMEs were fast and there were large flares associated with the main CMEs (and with the preceding CMEs in the case of the 2003 March 18 event). Nonetheless, the proton flux at

Table 2
Properties of the Preceding CMEs for the SEP Events Listed in Table 1

SEP No. (1)	SEP Date (2)	CME Onset (3)	CPA (deg) (4)	WD (deg) (5)	Speed (km s^{-1}) (6)	Flare Class (7)	Flare Onset (8)	Type II (Metric) (9)	Type II (DH) (10)	Database[c] (11)
2	1997 Nov 6	04:20	263	59	307	C1.9	03:12	03:28	n	CDAW
3	1998 May 2	05:31	Halo	360	542	C5.4	04:48	n	n	CDAW
4	1998 May 6	00:02	274	110	786	M2.5	23:27	23:42	n	CDAW
5	1999 Jun 4	00:50	Halo	360	803	-	-	n	n	CDAW
6	2000 Apr 4	15:06	271	52	619	-	-	n	n	CACTus
7	2000 Jun 10	10:17	297	200	1011	-	-	n	n	CACTus
8	2000 Jul 14	08:54	245	12	395	C7.1	06:52[b]	n	n	SEEDS
10	2000 Sep 12	08:06	190	31	344	-	-	n	n	SEEDS
11	2000 Oct 25	04:06	243	60	459	-	-	n	n	CDAW
12	2000 Nov 8	17:06	252	42	391	M2.9	16:22	n	n	CDAW
13	2000 Nov 24	11:54	337	45	796	C2.4	11:34	n	n	CDAW
14	2001 Jan 28	09:30	270	79	638	-	-	n	n	CDAW
17	2001 Apr 10	02:06	268	54	539	-	-	n	n	CDAW
19	2001 Apr 15	11:18	199	70	511	C5.3	10:56	n	n	CDAW
21	2001 Oct 1	01:54	226	68	478	-	-	n	n	CDAW
22	2001 Oct 19	15:06	255	14	502	-	-	n	n	SEEDS
23	2001 Nov 4	14:10	302	110	844	-	-	n	n	CACTus
25	2001 Nov 23	21:30[a]	308	43	733	-	-	n	n	SEEDS
26	2001 Dec 26	02:06	283	21	800	-	-	n	n	CDAW
28	2002 Feb 20	03:30	306	54	813	M4.2	02:44	03:13	n	CDAW
30	2002 Mar 18	20:06	184	153	823	-	-	n	n	CDAW
33	2002 May 22	00:06	230	186	1246	-	-	n	00:00	CDAW
34	2002 Jul 16	20:30[a]	Halo	360	1151	X3.0	19:59	n	n	CDAW
36	2002 Aug 22	17:30[a]	219	17	464	C4.8	17:20[b]	n	n	CDAW
37	2002 Aug 24	20:50[a]	262	131	861	-	-	n	n	CDAW
38	2002 Sep 6	23:30[a]	212	60	666	-	-	n	n	CDAW
39	2002 Nov 9	10:56	199	224	1115	-	-	n	n	CACTus
40	2003 May 28	23:50[a]	Halo	360	964	X1.3	22:56	23:06	n	CDAW
41	2003 May 31	00:30	306	73	765	-	-	n	n	CDAW
44	2003 Nov 2	08:30	218	95	354	M1.0	06:59	n	n	SEEDS
45	2003 Nov 2	09:30	Halo	120	2036	-	-	n	n	CDAW
46	2003 Nov 4	12:06	Halo	360	1208	C5.7	11:15	n	n	CDAW
47	2003 Nov 20	02:50	221	63	364	M1.4	01:47	n	n	CDAW
48	2003 Dec 2	05:50	293	11	756	-	-	n	n	CDAW
50	2004 Jul 25	13:31	245	16	556	C2.1	13:18	n	n	CDAW
51	2004 Nov 7	09:54	325	30	467	C6.7	09:35[b]	n	n	CDAW
53	2005 Jan 16	14:54[a]	222	271	498	-	-	14:16	n	CDAW
54	2005 Jan 17	09:30	Halo	110	2094	X2.2	09:06	09:16	09:25	CDAW
55	2005 Jan 20	04:06	301	18	503	C4.8	03:21	n	n	CDAW
56	2005 Jul 13	12:54	275	49	471	M3.2	12:03	n	n	CDAW
57	2005 Aug 22	14:18	214	10	414	-	-	n	n	CACTus
58	2006 Dec 13	20:28[a]	193	50	474	-	-	n	n	CDAW
59	2006 Dec 14	20:30	237	16	316	-	-	n	n	CDAW
60	1998 Apr 20	03:16	237	43	316	-	-	n	n	CDAW
61	1998 May 9	02:35	258	69	768	M3.1	01:49	n	n	SEEDS
62	1999 Apr 24	11:06	220	36	1026	-	-	n	n	CDAW
63	1999 Jun 1	13:25	307	105	300	-	-	n	n	CDAW
64	2000 Feb 18	08:54	235	44	1004	-	-	n	n	SEEDS
66	2000 Oct 16	06:26	267	150	441	C7.0	05:32	n	n	SEEDS
67	2001 Apr 18	18:54	250	10	606	-	-	n	n	SEEDS
68	2001 May 7	10:06	214	233	604	-	-	n	n	CDAW
69	2001 Jun 15	07:31	220	45	306	-	-	n	n	SEEDS
71	2002 Mar 22	11:06	Halo	130	1750	M1.6	10:12	10:47	11:30	CDAW
72	2002 Jul 7	04:06	282	44	375	-	-	n	n	CDAW
73	2004 Nov 1	03:54	242	192	459	-	-	03:21	n	CDAW
74	2005 Jul 14	07:54	266	103	752	-	-	n	n	CDAW
75	2005 Jul 17	09:54	283	47	652	-	-	n	n	CDAW

Notes.
[a] Time corresponds to previous day.
[b] The flare may be not associated with the corresponding CME because the waiting time between them is below 20 minutes or above 2 hr.
[c] The source database: if the CME is identified by more than one database, CDAW is given priority.

Table 3
Properties of the Main CMEs in Group III

No.	Date	CME	CPA (deg)	WD (deg)	Speed (km s^{-1})	AR[a]	loc.	FC[b]	Flare	Type II (Metric)	Type II (DH)	Δt[c] (hr)	Com.[d]	Pre-flare (FC/Δt_1)
(1)	(2)	(3)	(4)	(5)	(6)	(7)	(8)	(9)	(10)	(11)	(12)	(13)	(14)	(15)
1	1998 Jun 5	07:01	205	132	1017	fp	S45W20	-	-	n	n	5.5	e	-/-
2	1999 Sep 9	21:54	345	103	1071	08682	N19W61	-	-	n	n	2.0	ne	-/-
3	1999 Sep 19	17:18	307	139	1144	08699	N21W71	-	-	n	n	6.4	e	C4.9/3.2
4	1999 Nov 16	06:54	270	77	1193	08759	N11W46	?	-	n	n	1.4	ne	-/-
5	2000 Feb 12	04:30	Halo	110	1107	08858	N24W38	M1.7	03:51	04:02	03:55	7.0	e	-/-
6	2000 Mar 4	09:54	351	61	955	08889	N20W46	-	-	n	n	7.0	ne	-/-
7	2000 May 15	16:26	257	165	1212	08993	S24W67	C7.6	15:45	n	n	2.0	e	-/-
8	2000 Jun 25	07:54	262	165	1617	09046	N16W55	M1.9	07:16	07:50	08:10	1.8	e	-/-
9	2000 Sep 16	13:50	198	100	1056	09165	N14W13	C2.2	13:07	n	n	8.5	e	C2.6/4.9
10	2000 Oct 26	11:50	321	97	964	09199	N17W77	-	-	n	n	4.0	e	C3.7/6.8
11	2000 Nov 24	22:06	Halo	360	1005	09236	N21W14	X1.8	21:43	21:52	22:24	6.6	hb	C2.3/3.8
12	2001 Apr 2	11:26	270	80	992	09393	N17W60	X1.1	10:58	11:10	11:30	5.6	e	X1.4/1.4
13	2001 Apr 5	09:06	283	205	1750	09401	N24W83	?	-	n	n	7.0	hb	M3.1/7.1
14	2001 Apr 26	12:30	Halo	360	1006	09433	N17W31	M7.8	11:26	n	12:40	4.0	e	C2.2/2.5
15	2001 Dec 18	18:30	255	103	1025	09739	S13W71	?	-	n	n	1.6	e?	-/-
16	2002 Mar 20	23:54	242	160	1075	09870	S20W60	C5.7	23:45	n	n	6.0	ne	C2.4/2.6
17	2002 Apr 30	23:26	254	199	1103	09914	N06W78	-	-	n	n	7.2	e	-/-
18	2002 May 22	00:06	230	186	1246	09948	S15W70[e]	?	-	n	00:00	8.0	ne	-/-
19	2002 Aug 3	19:31	259	138	1150	10039	S16W76	X1.0	18:59	n	19:20	2.0	e	-/-
20	2002 Aug 16	06:06	293	162	1378	10061	N07W83	M2.4	05:46	05:52	06:15	7.6	e	-/-
21	2002 Aug 20	08:54	237	122	1099	10069	S10W38	M3.4	08:22	n	n	7.0	e	C4.0/3.7
22	2002 Nov 11	15:53	212	93	1083	10180	S07W59	M1.8	15:11	16:04	n	8.0	ne	C6.5/1.3
23	2003 Mar 18	12:30	263	209	1601	10314	S15W46	X1.5	11:50	12:16	12:25	5.0	e	C2.1/5.9
24	2003 Mar 19	02:30	Halo	360	1342	10314	S16W56	-	-	02:22	02:30	1.0	ne?	C1.5/0.9
25	2003 Oct 27	08:30	265	144	1322	10484	N03W48	M2.7	07:50	n	n	4.0	e	M1.2/4.3
26	2003 Nov 3	10:05	293	103	1420	10488	N08W77	X3.9	09:43	09:50	10:00	8.1	hb	X2.7/8.9
27	2005 May 6	03:30	280	109	1120	10756	S04W71	C9.3	03:05	n	n	5.6	e	C7.8/7.4
28	2005 May 6	11:54	277	129	1144	10756	S04W76	M1.3	11:11	n	n	8.4	e	C2.2/6.5
1	2000 Jun 17	23:10	263	70	927	?	?	C4.6	22:27	n	n	2.3	x,e	-/-
2	2002 Oct 25	18:06	336	132	1030	10162	N28W11	M1.5	17:22	17:40	n	3.0	x,ne	C1.6/1.6

Notes.
[a] "fp" denotes no NOAA active region number and possibly a filament/prominence eruption.
[b] "-" denotes that no flares are identified; "?" denotes that flare brightening was seen, but no flare information was given at http://www.SolarMonitor.org.
[c] The time interval between main CME and preceding CME.
[d] "e" denotes events that show enhancement in low-energy channels of ULEIS/*ACE* and/or weak enhancement in high-energy channels of SIS/*ACE*. Some of them show weak enhancement in >10 MeV channel of *GOES* but not larger than 10 pfu; "hb" denotes events that have high background level in >10 MeV channel of *GOES* and show no clear flux increases; "ne" denotes events that have no enhancement in all energy channels; "x" denotes events that have in sufficient EIT information.
[e] Cited from Shen et al. (2006).

>10 MeV nucleon^{-1} did not exceed 10 pfu. Finally, there were seven events that showed no enhancements at the *ACE*/ULEIS energies. Four of them (1999 September 9, 1999 November 16, 2000 March 4, and 2002 May 22) had no preceding flares and three of them (2002 March 20, 2002 November 11, and 2003 March 19) had preceding flares.

2.4. Single CMEs with no SEPs

We now examine single CMEs that do not lead to large SEP events. We select the single CMEs from the CDAW database using the following criteria: (1) the speed is faster than 900 km s^{-1}, (2) the angular width is larger than 60°, and (3) the source location is on the western hemisphere with a longitude smaller than 90°.

A total of 39 single western CMEs are identified using these criteria. These are shown in Table 5. In Table 5, Column 1 is the event number, Column 2 is the event date, and Column 3 is the CME onset time. Columns 4–6 are the CPA, WD, and speed of the CMEs, respectively. Columns 7 and 8 are the active source region (AR) number and its location. Columns 9 and 10 are the flare class and the flare onset time. Columns 11 and 12 are the onset times of metric type II and DH type II radio bursts. Column 13 contains comments. Column 14 is the closest preceding flares identified within 9 hr.

In terms of CME properties, these CMEs are very similar to those in Table 1. For example, 21 of these CMEs have metric type II radio bursts; 4 have *X*-class associated flares, and 18 have *M*-class flares. However, none of them has preceding CMEs within 9 hr.

Compared to the 16 group II events (i.e., single CMEs leading to large SEP events) in Table 1, some of these CMEs show signatures of producing particles up to a few MeV nucleon^{-1} which are observed by the low-energy channels of *ACE*/ULEIS. These are labeled as "e" in Column 13 of Table 5. There were also four CMEs which appeared to have no clear flaring activities. They were probably due to prominence or filament eruption and are labeled by "fp" in Column 7 of Table 5.

Of the 39 events, 16 events were observed to have preceding flares within 9 hr of the main CME. Ten of them

Table 4
Properties of Preceding CMEs in Group III

No.	Date	CME Onset	CPA (deg)	WD (deg)	Speed (km s^{-1})	FC	Flare Onset	Type II (Metric)	Type II (DH)	Database
(1)	(2)	(3)	(4)	(5)	(6)	(7)	(8)	(9)	(10)	(11)
1	1998 Jun 5	01:30	217	57	478	-	-	n	n	CDAW
2	1999 Sep 9	19:52	304	73	603	-	-	n	n	CDAW
3	1999 Sep 19	10:54	289	5	408	C3.2	10:34	n	n	SEEDS
4	1999 Nov 16	05:30	285	129	712	-	-	n	05:17	CDAW
5	2000 Feb 11	21:30	328	14	799	-	-	n	n	CACTus
6	2000 Mar 4	03:57	335	60	882	-	-	n	n	CDAW
7	2000 May 15	14:26	262	49	721	-	-	n	n	CDAW
8	2000 Jun 25	06:06	267	5	368	-	-	n	n	CDAW
9	2000 Sep 16	05:17	Halo	360	1215	M5.9	04:05	n	04:30	CDAW
10	2000 Oct 26	07:50	292	32	930	-	-	n	n	CDAW
11	2000 Nov 24	15:30	Halo	360	1245	X2.3	14:51	n	15:25	CDAW
12	2000 Apr 2	05:50	285	9	628	M1.0	05:25	n	n	CDAW
13	2001 Apr 5	02:06	285	52	1857	C4.4	01:29	n	n	CDAW
14	2001 Apr 26	08:30	332	91	740	-	-	n	n	CDAW
15	2001 Dec 18	16:54	250	33	573	-	-	n	n	CDAW
16	2002 Mar 20	17:54	Halo	360	603	-	-	n	n	CDAW
17	2002 Apr 30	16:11	266	28	559	-	-	n	n	CDAW
18	2002 May 21	16:06	269	48	603	-	-	n	n	SEEDS
19	2002 Aug 3	17:30	274	86	889	-	-	n	n	CACTus
20	2002 Aug 15	22:30	301	68	857	-	-	n	n	CDAW
21	2002 Aug 20	01:54	244	157	961	M5.0	01:33	n	n	CDAW
22	2002 Nov 11	07:54	217	36	1225	M2.9	07:25	n	n	CDAW
23	2003 Mar 18	07:30	204	71	619	M2.5	05:51	n	n	CDAW
24	2003 Mar 19	01:31	214	65	775	-	-	n	n	CDAW
25	2003 Oct 27	04:30	303	48	481	M1.2	04:12[a]	n	n	CDAW
26	2003 Nov 3	01:59	304	65	827	X2.7	01:09	n	01:15	CDAW
27	2005 May 5	21:53	271	56	868	-	-	n	n	CACTus
28	2005 May 6	03:30	280	109	1120	C9.3	03:05	n	n	CDAW
1	2000 Jun 17	20:50	254	14	538	-	-	n	n	SEEDS
2	2002 Oct 25	15:06	Halo	360	870	-	-	n	n	CDAW

Note. [a] Uncertain association of the flare with the CME because their time separation is either below 20 minutes or above 2 hr.

(62.5%) showed some enhancements at the *ACE*/ULEIS and/or *ACE*/SIS channels, and the remaining 6 (the 1997 July 25, 2001 April 11, 2001 October 25, the 2002 July 18, the 2002 November 10, and the 2005 January 19 events) showed no enhancements. Four of these six events had high background intensity (>10 pfu) at *GOES* >10 MeV channel prior to the SEP.

For the remaining 23 events where no preceding flares were identified, 13 of them (57%) showed some enhancements at the *ACE*/ULEIS and/or *ACE*/SIS channels from background and 10 showed no enhancements. This suggests that single CMEs (whether or not there are preceding flares) can lead to some energization and enhancement of particles at the energy range of the *ACE*/ULEIS and/or the *ACE*/SIS channels, while the presence of preceding flares slightly increases such a probability (62.5% versus 57%).

3. RESULTS

Tables 1–5 are the main results of this paper. In Figure 1, we plot the number of CMEs in each group in a pie plot. There are 71 twin CMEs and 55 single CMEs. Some useful statistics can be immediately obtained from Figure 1. Considering group I and group II, we find that 73% (43 out of 59) of large SEP events are of "twin CME" in nature. Considering group I and group III, we find that 61% (43 out of 71) of "twin" CMEs will lead to large SEP events at the Earth. In comparison, from group II and group IV, only 29% (16 out of 55) of single CMEs will lead to large SEP events at the Earth.

These results indicate that there is a strong correlation between twin CMEs and large SEP events.

Note, however, in Table 1 that 16 out of 59 western events had no preceding CMEs. This suggests that single CMEs, under favorable conditions, can still lead to large SEP events. Since the flare size and the CME speed are two good indicators of the amount of free magnetic field energy that is released during an SEP event, we examine possible correlations between the peak proton flux and the corresponding flare size or the CME speed. Figure 2 and Figure 3 are the scatter plots of the peak >10 MeV proton flux as a function of flare size and CME speed for all 59 western events in Table 1, respectively.

If we consider all events (Group I and Group II) together, we find that there is neither a good correlation between the flare size and the SEP intensity, nor between the CME speed and the SEP intensity. This agrees with previous studies. Gopalswamy et al. (2004) found that "while the average flare size was larger for high-intensity SEP events, the SEP intensity showed poor correlation with the flare size." Kahler (1996) has shown that although the maximum energy and the intensity of energetic particles in SEP events are generally correlated with shock speed, the scatter is very large.

If we consider only the 16 single-CME events (group II), although the scattering is still large, there seems to a be general trend that one tends to find larger SEP events for larger flares and/or fast CMEs. No such trend exists for events in group I.

Table 5
Properties of CMEs in Group IV

No.	CME Date	CME Onset	CPA (deg)	WD (deg)	Speed (km s^{-1})	AR[a]	Loc.	FC[b]	Flare Onset	Type II (Metric)	Type II (DH)	Com.[c]	Pre-flare (FC/Δt_1)
(1)	(2)	(3)	(4)	(5)	(6)	(7)	(8)	(9)	(10)	(11)	(12)	(13)	(14)
1	1998 Jan 3	09:42	290	85	1020	08126	N20W64	-	-	n	n	e	-/-
2	1999 Jun 27	09:06	349	86	903	08592	N23W25	M1.0	08:34	08:42	n	e	-/-
3	1999 Jun 28	21:30	336	184	903	08592	N22W46	C3.5	20:55	20:56	21:03	ne	-/-
4	1999 Jul 25	13:31	Halo	360	1389	08639	N38W81	M2.4	13:07	13:21	n	ne	C3.9/5.2
5	1999 Aug 28	01:26	289	98	1147	08674	S24W29	M2.8	00:50	n	n	e	C5.5/4.1
6	1999 Sep 23	15:54	262	77	1150	fp	S25W50	-	-	n	n	ne	-/-
7	2000 Jan 5	01:53	352	127	1399	08816	N23W28	C2.4	01:17	n	n	ne	-/-
8	2000 Jan 28	20:12	Halo	360	1177	08841	S31W17	C4.7	19:45	n	20:20	e	-/-
9	2000 May 5	15:50	Halo	120	1594	08976	S12W88	M1.5	15:18	n	16:35	e	C1.2/6.3
10	2000 Jun 15	20:06	298	116	1081	09041	N20W65	M1.8	19:37	19:42	19:52	e	C2.6/4.4
11	2000 Jun 28	19:31	270	134	1198	fp	N24W85	-	-	18:57	n	e	-/-
12	2000 Sep 16	05:18	Halo	360	1215	09165	N15W07	M5.9	04:06	04:11	04:30	e	M5.9/1.2
13	2001 Jan 14	06:30	327	134	945	fp	N60W10	-	-	n	n	ne	-/-
14	2001 Jan 26	12:06	276	176	928	09320	S23W57	C1.6	11:50	11:57	12:06	e	-/-
15	2001 Feb 11	01:31	Halo	80	1183	09334	N24W57	-	-	01:03	01:40	e	-/-
16	2001 Apr 9	15:54	Halo	360	1192	09415	S21W04	M7.9	15:20	15:26	15:53	e	C6.1/6.6
17	2001 Apr 11	00:54	242	69	939	09417	S08W48	M1.0	00:24	n	n	ne,hb	C3.3/2.6
18	2001 Apr 11	13:31	Halo	360	1103	09415	S23W32	M2.3	12:56	13:17	13:15	e,hb	C2.2/1.7
19	2001 May 10	01:31	246	198	1056	09445	N25W80	C5.6	01:04	n	n	ne	-/-
20	2001 Jul 19	10:30	275	166	1668	09537	S08W62	M1.8	09:52	n	n	ne	-/-
21	2001 Oct 25	15:26	Halo	360	1092	09672	S16W21	X1.3	14:41	14:47	15:30	ne	C2.2/1.6
22	2002 May 7	00:06	287	100	1222	09929	N22W66	C6.4	23:53	n	n	e	-/-
23	2002 Jul 18	08:06	Halo	360	1099	10030	N19W30	X1.8	07:24	07:42	07:55	ne,hb	C1.7/1.3
24	2002 Aug 6	18:25	218	134	1098	fp	S38W18	-	-	n	n	ne	-/-
25	2002 Nov 10	03:30	203	282	1670	10180	S12W37	M2.4	03:04	03:14	03:20	ne,hb	C5.8/4.3
26	2002 Dec 19	22:06	Halo	120	1092	10229	N15W09	M2.7	21:33	n	21:45	e	-/-
27	2002 Dec 22	03:30	328	272	1071	10223	N23W42	M1.1	02:14	n	04:20	e	C1.2/5.8
28	2003 Jan 27	22:23	205	267	1053	10267	S17W23	-	-	22:11	22:20	ne	-/-
29	2003 Mar 17	19:54	291	96	1020	10314	S14W39	X1.5	18:50	n	n	e	C7.7/3.3
30	2003 Nov 7	15:54	Halo	360	2237	10495	S21W89	-	-	n	n	e,hb	-/-
31	2003 Nov 11	13:54	Halo	360	1315	10498	S04W63	M1.6	13:21	13:33	n	ne	-/-
32	2004 Apr 8	10:30	Halo	360	1068	10588	S15W11	C7.4	09:52	10:05	10:25	e	C1.2/8.8
33	2004 Nov 9	17:26	Halo	130	2000	10696	N08W51	M8.9	16:59	17:18	17:35	e,hb	-/-
34	2004 Dec 3	00:26	Halo	360	1216	10708	N08W02	M1.5	23:44	23:52	00:07	e	-/-
35	2005 Jan 4	09:30	288	102	1087	fp	N15W60	-	-	n	n	ne	-/-
36	2005 Jan 19	08:29	Halo	360	2020	10720	N15W51	X1.5	08:03	08:11	09:20	ne,hb	M7.4/1.5
37	2005 Feb 17	00:06	Halo	360	1135	10734	S03W24	-	-	n	n	e	C1.1/4.6
38	2005 Jul 9	22:30	Halo	360	1540	10786	N12W28	M2.8	21:47	21:59	22:15	e	-/-
39	2005 Aug 22	01:31	Halo	360	1194	10798	S11W54	M2.6	00:44	00:53	n	e	-/-

Notes.
[a] "fp" denotes no NOAA active region number and possibly a filament/prominence eruption.
[b] "-" denotes that no flares are identified.
[c] "e" denotes events that show enhancement in low-energy channels of ULEIS/*ACE* and/or weak enhancement in high-energy channels of SIS/*ACE*. Some of them show weak enhancement in >10 MeV channel of *GOES* but not larger than 10 pfu; "hb" denotes events that have high background level (>10 pfu) in >10 MeV channel of *GOES*; "ne" denotes events that have no enhancement in all energy channel.

This can be easily understood in the "twin-CME" scenario: in the "twin-CME" scenario, the presence of the first CME can set up a favorable environment for efficient particle acceleration at the second CME-driven shock, therefore weakening any dependence of the peak intensity on the flare size and CME speed if there was any.

Also note that there seems to be a separation of group I (blue crosses) events from group II (red dots) events in Figures 2 and 3. For example, for events with similar flare classes in Figure 2, the SEP peak intensities of "twin-CME" events tend to be larger than those of single CMEs. In addition, we note that 29 of 43 "twin-CME" events have peak intensity >100 pfu. In comparison only 5 of 16 single-CME events have peak intensity >100 pfu. Therefore the probability of "twin-CME" events causing extreme large SEP events (such as events with peak intensity >100 pfu) is significantly higher than single CMEs.

As suggested by Li & Zank (2005), one favorable condition that the "twin-CME" scenario can provide for a more efficient acceleration at the second shock is the creation of the seed population. Therefore it is an interesting question to ask whether or not the eruption environments in those 16 single-CME events in Table 1 have an enhancement of seed population. Unfortunately, remotely examining the seed population of these events (and in all large SEP events) is hard if not impossible. Nevertheless, at least for western events, we can obtain some crude information

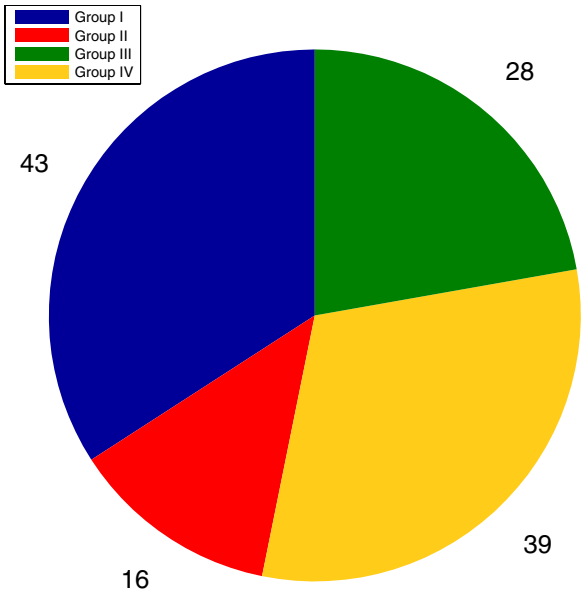

Figure 1. Fast CMEs ($v > 900$ km s^{-1}) with a western source region and a width of $>60°$ identified in our study. CMEs in group I have preceding CMEs (in 9 hr) and lead to a large SEP at the Earth. CMEs in group II have no preceding CMEs (in 9 hr) and lead to a large SEP at the Earth. CMEs in group III have preceding CMEs (in 9 hr) and lead to no large SEPs at the Earth. CMEs in group IV have no preceding CMEs (in 9 hr) and lead to no large SEPs at the Earth.

(A color version of this figure is available in the online journal.)

about the seed population through in situ measurements by, for example, the ULEIS instrument onboard the *ACE* spacecraft. Assuming the ULEIS observation of the 0.64–1.28 MeV proton channel 1 day prior to a large SEP event can be regarded as a proxy for the close-to-the-Sun environment, then one can examine the correlation between an SEP event's peak flux and the pre-event (1 day prior) seed population.

Figure 4 is a scatter plot of the peak flux and the seed population for all 59 western events from Table 1. The x-axis is the 1 day prior daily average proton intensity from the ULEIS/*ACE* 0.64 to 1.28 MeV channel. The y-axis is the >10 MeV peak proton flux measured by the *GOES* spacecraft. Events identified as "np" in Table 1 are denoted by red dots in Figure 4, and events associated with the "twin-CME" scenario in Table 1 are denoted by blue crosses. For comparison, the median 1 day prior daily average proton intensity of the 0.64–1.28 MeV channel for all 59 events, which is 76 pfu, and the median daily average proton intensity of the 0.64–1.28 MeV channel for the period 1998–2006, which is 1.66 pfu, are also shown as the two arrows in the figure.

From the figure, we can see that for events without preceding CMEs, there seems to be a ceiling (denoted by the dashed pink line) for the SEP peak intensity. For events with preceding CMEs (the blue crosses), however, the event peak flux and the pre-event seed particle flux at 1 AU has no correlation. This can be understood naturally within the "twin-CME" scenario: for events marked by blue crosses, since the presence of the preceding CME (and the preceding flares) can provide the seed particles for the second CME, there is no need to have these seed particles 1 day prior to the event.

We do note that because the ULEIS measurement is at 1 AU, it can only serve as a proxy, and does not necessarily reflect the pre-event plasma environment close to the Sun. Indeed, for an ion of energy 0.2 MeV nucleon^{-1}, the free-streaming travel time (assuming zero pitch angle) from the Sun to the Earth, for a 1.2 nominal Parker spiral, is ~8.0 hr. In 8 hr, the Sun rotates by ~4° and the footpoint of the field line that connects to the Earth may change significantly. Note that, as in Figures 2 and 3, a separation of group I (blue crosses) events from group II (red dots) events can also be seen in Figure 4.

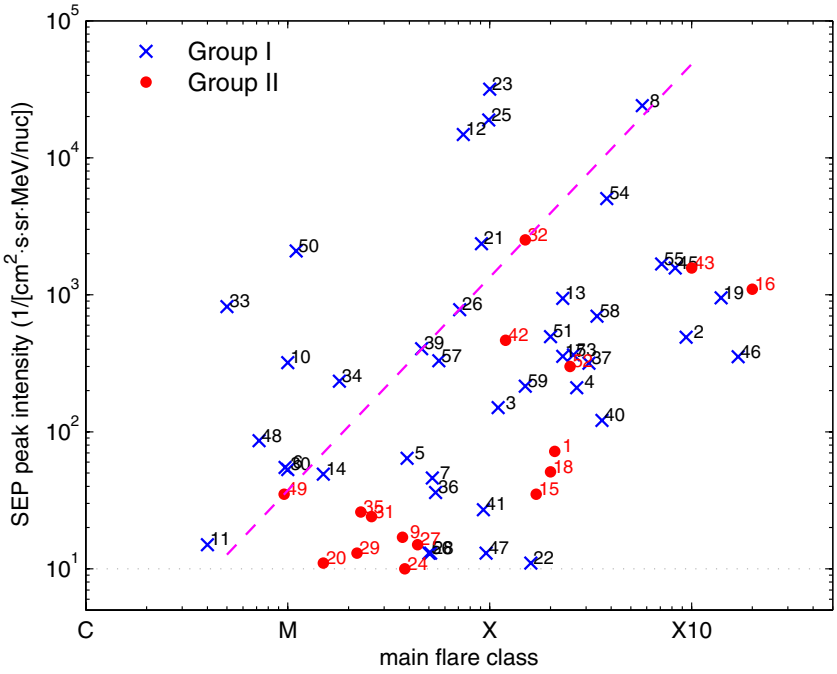

Figure 2. Peak flux of all 59 western events from Table 1. The x-axis is the corresponding flare class. The y-axis is the >10 MeV peak proton flux measured by the *GOES* spacecraft. Events identified as "twin-CME" scenario in Table 1 are labeled as blue crosses (group I) and events identified as "np" in Table 1 are labeled as red dots (group II).

(A color version of this figure is available in the online journal.)

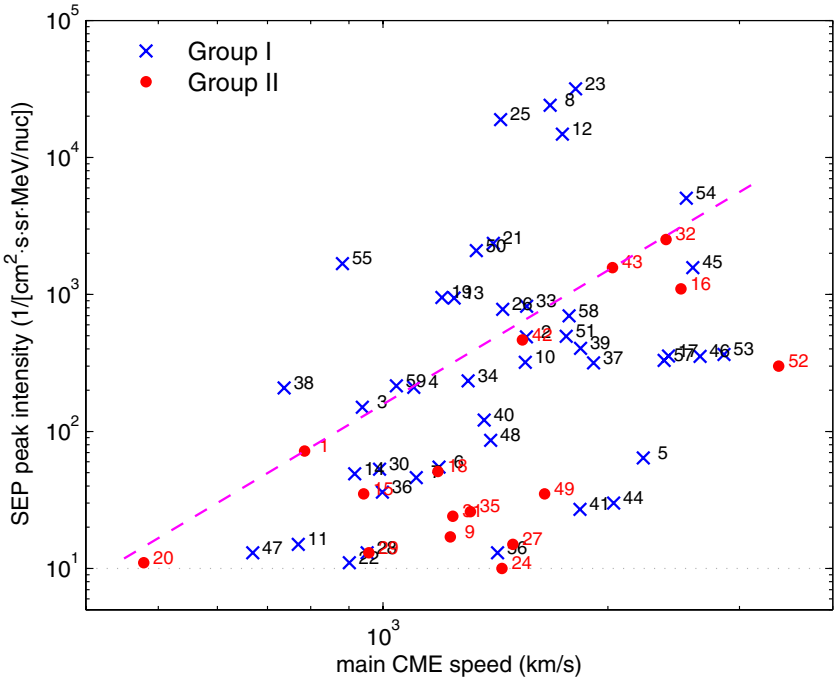

Figure 3. Peak flux of all 59 western events from Table 1. The *x*-axis is the corresponding CME speed. The *y*-axis is the >10 MeV peak proton flux measured by the *GOES* spacecraft. Events identified as "twin-CME" scenario in Table 1 are labeled as blue crosses (group I) and events identified as "np" in Table 1 are labeled as red dots (group II).

(A color version of this figure is available in the online journal.)

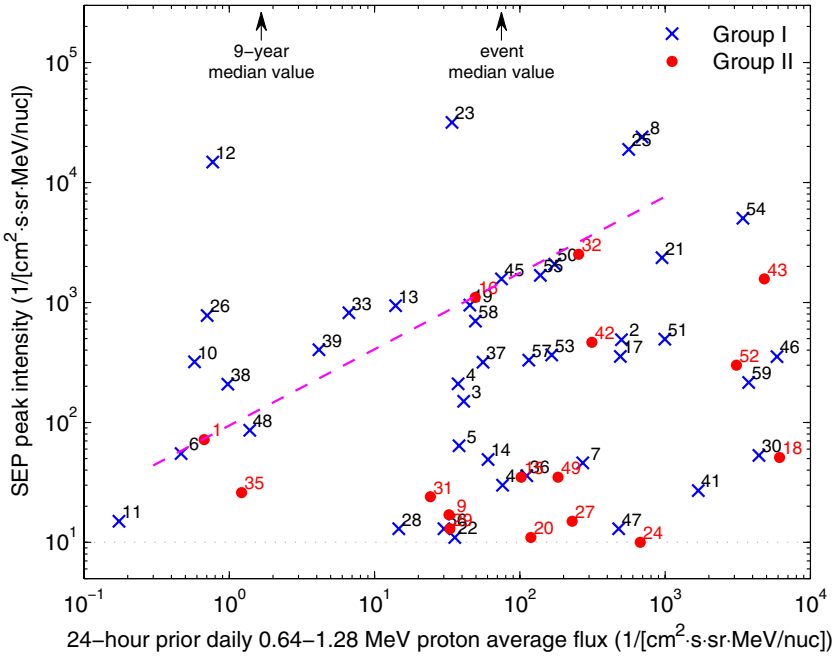

Figure 4. Peak flux of all 59 western events from Table 1. The *x*-axis is the 1 day prior daily average proton intensity from the *ACE*/ULEIS 0.64 to 1.28 MeV channel. The *y*-axis is the >10 MeV peak proton flux measured by the *GOES* spacecraft. Events identified as "twin-CME" scenario in Table 1 are labeled as blue crosses (group I) and events identified as "np" in Table 1 are labeled as red dots (group II). The arrows indicate the median values of 1 day prior daily average proton intensity of all 59 events and of daily average proton intensity from 1998 to 2006 in the 0.64–1.28 MeV channel.

(A color version of this figure is available in the online journal.)

Figures 2–4 are very important results of this study. They show that for large SEP events where a preceding CME exists within 9 hr, neither flare size, nor CME speeds, nor 1 day prior seed populations are deciding factors for the size of the proton peak intensity of the event, consistent with the "twin-CME" scenario.

3.1. Statistical Analyses

We first consider the time interval between the preceding CME and the main CME for "twin-CME" events. Figure 5 shows the histogram of time intervals between the main CMEs and the preceding CMEs in group I. The distribution of the

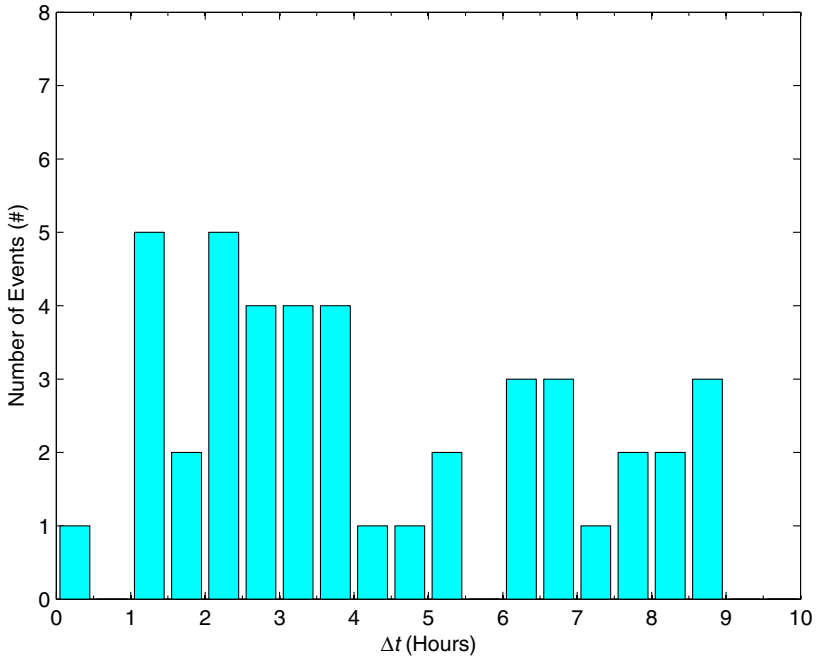

Figure 5. Histogram of the distribution of time intervals between the main CMEs and the preceding CMEs for events identified as "twin CME" in Table 1 with a source region in the western hemisphere and longitude <90° (denoted as group I in the text).

(A color version of this figure is available in the online journal.)

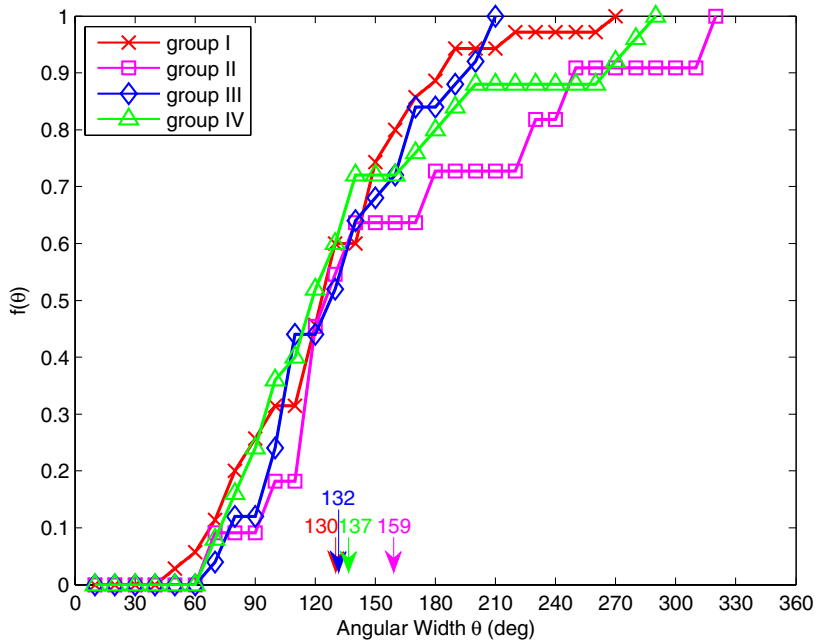

Figure 6. "Integrated percentage" function $f(\theta)$. The red curve is for the main CMEs in group I, the magenta curve is for the single CMEs in group II, the blue curve is for the main CMEs in group III, and the green curve is for the single CMEs in group IV. See the text for details.

(A color version of this figure is available in the online journal.)

interval is relatively flat. Out of 43 events, 26 have intervals shorter than 4.5 hr and 17 have intervals longer than 4.5 hr.

We next discuss the angular width of the main CMEs in groups I and III, and the fast single CMEs in groups II and IV. These widths are listed in Tables 1, 3, and 5. Using an angular bin of 10°, we plot the cumulative angular distribution function $f(\theta)$ in Figure 6. The y-axis of Figure 6, $f(\theta_i)$, represents the percentage of events having width $\theta < \theta_i$. Note that we do not include halo CMEs with no angular width information in Figure 6 (and Figure 7 below).

The red curve with "×" is for group I, the magenta curve with rectangles is for group II, the blue curve with diamonds is for group III, and the green curve with triangles is for group IV. We can see from Figure 6 that the angular width distributions for the main CMEs in group I and group III (red and blue curves) are very similar. Also note that CMEs in group II appear wider than those in the other three groups. However the sample size for group II is small. There are a total of 16 events in group II and 5 of them have no angular width information. Overall, the angular width of a fast CME does not seem to be a good indicator of a large SEP event.

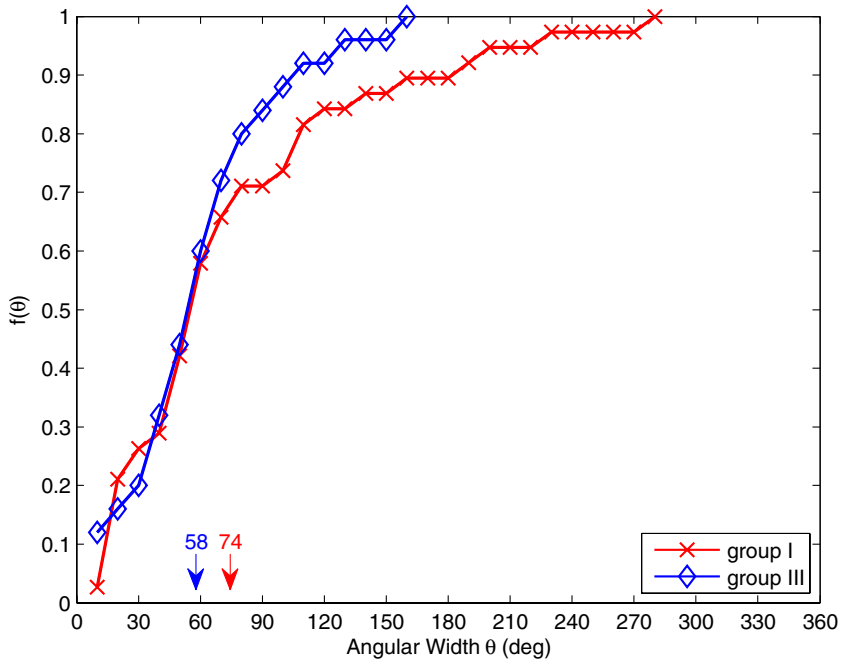

Figure 7. Same as Figure 6, but for the preceding CMEs in groups I and III.
(A color version of this figure is available in the online journal.)

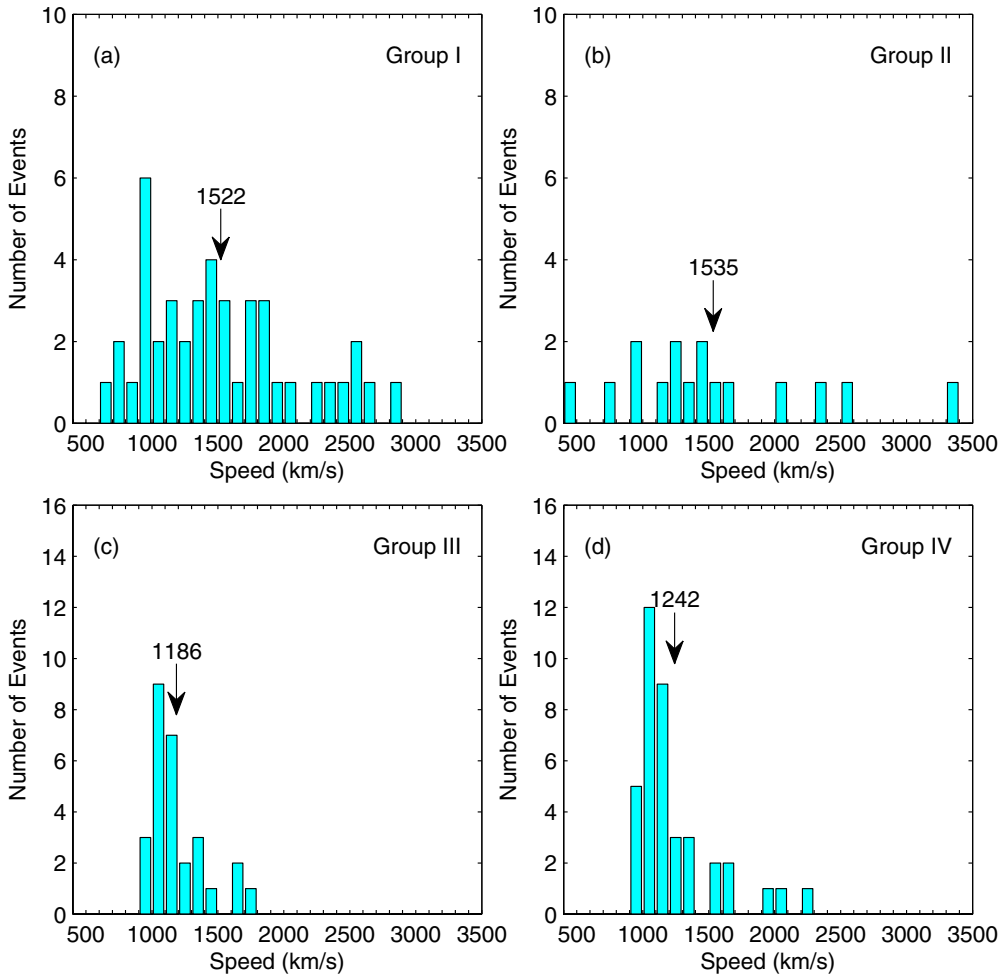

Figure 8. Histograms of speed of (a) the main CMEs in group I, (b) the "single CMEs" in group II, (c) the main CMEs in group III, and (d) the single CMEs in group IV. Each bin is 100 km s^{-1} for all panels. The arrows and numbers indicate the average values.
(A color version of this figure is available in the online journal.)

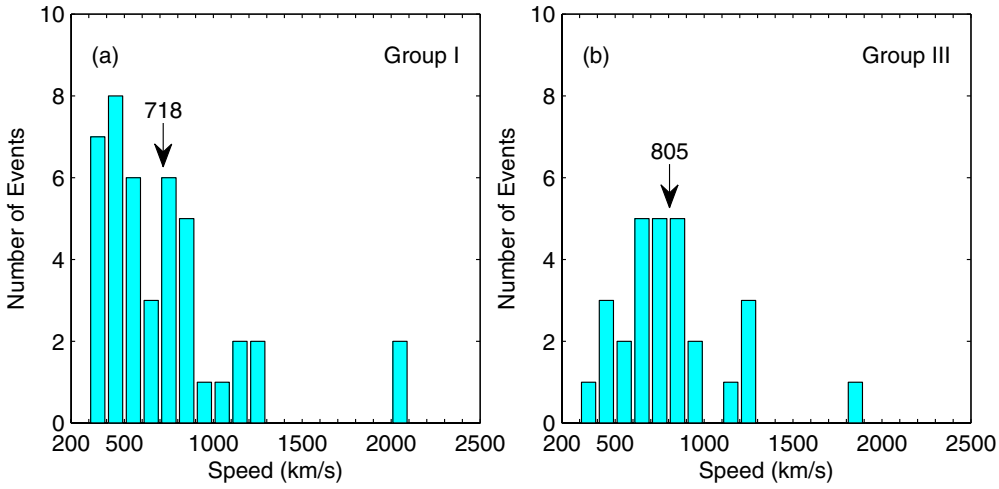

Figure 9. Same as Figure 8, but for preceding CMEs in group I and group III.
(A color version of this figure is available in the online journal.)

Figure 7 plots $f(\theta)$ for the preceding CMEs for group I and group III. Compared to Figure 6, the width of the preceding CMEs is a lot smaller than those of the main CMEs. The preceding CMEs in group I are also wider than the preceding CMEs in group III. This can be seen from Figure 7 where the red curve (group I) is to the right of the blue curve (group III). The average angular width for preceding CMEs in group I is 74° and that for group III is 58°.

Next, we plot in Figure 8 the speeds of the main CMEs in group I and group III, and of the single CMEs in group II and group IV. Panel (a) is for the main CMEs in group I. The average speed is 1522 km s^{-1}, comparable to the value of 1623 km s^{-1} obtained in Gopalswamy et al. (2010) and 1492 km s^{-1} in Gopalswamy et al. (2004) for large SEP events. Panel (b) is for group II, with an average of 1535 km s^{-1}. Panel (c) is for the main CMEs in group III, with an average value of 1186 km s^{-1}, slower than that of group I. Panel (d) is for group IV, with an average of 1242 km s^{-1}. The average speeds of the main CMEs for group I and group II are higher than those of the other two groups. However, their spread is also broader. Therefore, a CME with a speed of 900 km s^{-1} can lead to a larger SEP event than a CME with a speed of 1500 km s^{-1}. The speed histograms of the preceding CMEs in group I and group III are shown in Figure 9. Panel (a) is for the preceding CMEs in group I and panel (b) is for the preceding CMEs in group III. The distributions in panels (a) and (b) are similar. Compared to the main CMEs, the preceding CMEs are slower. The average speed for preceding CMEs in group I is 718 km s^{-1} and that for group II is 805 km s^{-1}. Clearly, the speed of the preceding CME is also not a trustworthy indicator of large SEP events.

Metric type II radio bursts are indicative of MHD shocks in the corona (for $r < 3\ R_{\odot}$). Since the "twin-CME" scenario suggests that the acceleration occurs close to the Sun, we have examined metric type II radio bursts in this study. In Figure 10, events with type II radio bursts detected are labeled by a "cross." Panel (a) is for the main CMEs in groups I and III and panel (b) is for the single CMEs in groups II and IV. We found that 30 of 43 (70%) of the main CMEs in group I have metric type II radio bursts, 14 of 16 (87.5%) of the CMEs in group II have metric type II radio bursts, 9 of 28 (32%) of the main CMEs in group III have metric type II radio bursts, and 21 of 39 (54%) of the CMEs in group IV have metric type II radio bursts. Also plotted in Figure 10 are the solar source locations as shown in Tables 1, 3, and 5.

Figure 11 plots the associated flare classes for the main CMEs in group I (panel (a)) and group III (panel (c)), and the single CMEs in group II (panel (b)) and group IV (panel (d)). For group I, the distribution is the broadest, with the smallest flare being C2.2 (the 2001 April 18 event) and the largest flare being X20 flare (the 2001 April 2 event). The median flare class is M9.6. The distributions of group II and group III are narrower, with a median of M7.8 and M2.4, respectively. The red bars in Figure 11 denote those events without clear flare identifications. Figure 12 plots the flare classes for the preceding CMEs in group I (panel (a)) and group III (panel (b)). The flare classes are generally smaller for the preceding CMEs. However, there are no clear differences between panel (a) and panel (b) of Figure 12.

The average flare class for events in groups I and II is larger than those of groups III and IV. This is consistent with the "Big Flare Syndrome" (Kahler 1982), which states that statistically energetic flare phenomena are more intense in larger flares, regardless of the detailed physics. However we note that the spreading of the flare class for group I and group II events is also larger than those of group III and group IV. Therefore, as in the case of the main CME speed (see Figure 8), the flare size of the main CME is not an accurate indicator of large SEP events. Our finding is consistent with the earlier work of Gopalswamy et al. (2004), who found that "while the average flare size was larger for high-intensity SEP events, the SEP intensity showed poor correlation with the flare size."

4. DISCUSSION AND CONCLUSION

In this work, we surveyed a total of 75 western large SEP events in solar cycle 23. Of these 75 events, 16 are limb events and 59 are disk events. For the 59 disk events, 43 (73%) have preceding CMEs with speed >300 km s^{-1} within 9 hr, and 16 have not. In two control studies, we also (1) identified 39 fast ($V > 900$ km s^{-1}) single western CMEs in solar cycle 23 (comparing to the 16 events shown in Table 1 that lead to large SEP events) that did not lead to large SEP events and (2) identified a total of 28 western "twin CMEs" in solar cycle 23 that did not lead to large SEP events. If we focus on western

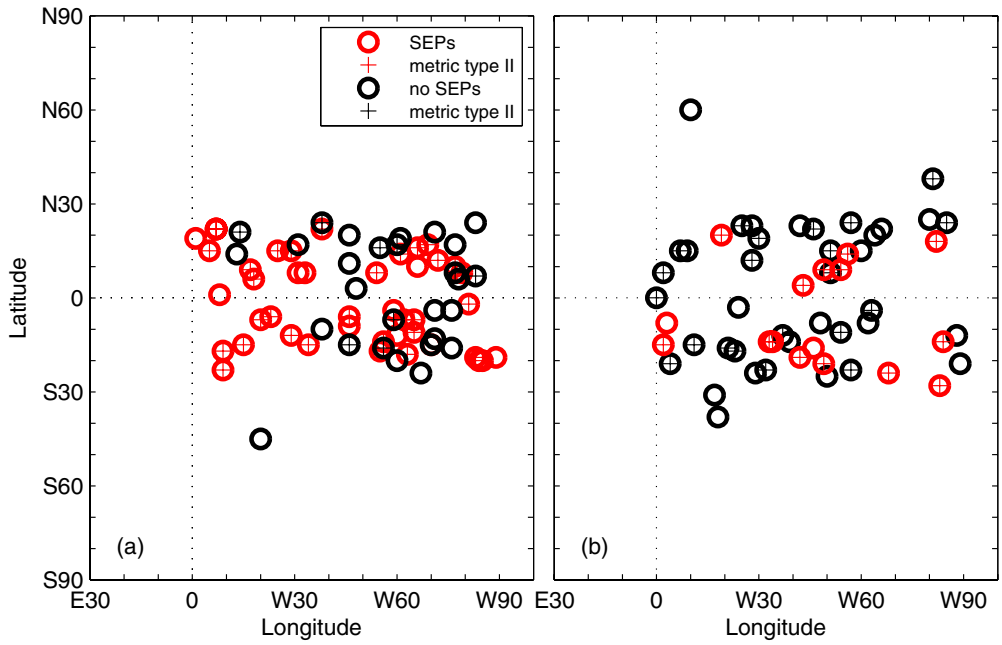

Figure 10. Scatter plots of source locations for (a) the "twin CMEs" and (b) the "single CMEs." The open red circles denote events with SEP events, and open black circles denote events with no SEP events. The cross symbols denote events with metric type II radio bursts.

(A color version of this figure is available in the online journal.)

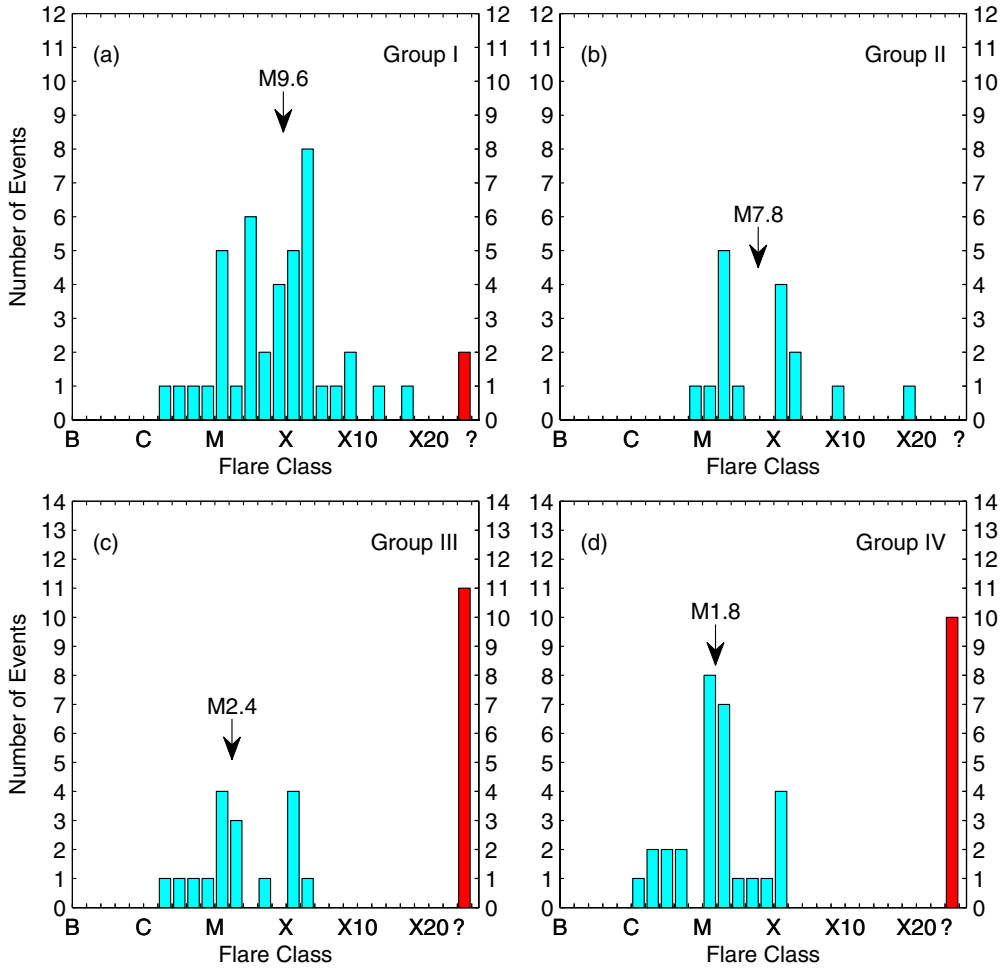

Figure 11. Histograms of flare classes for (a) the main CMEs of group I, (b) the "single CMEs" of group II, (c) the main CMEs of group III, and (d) the single CMEs of group IV. Red bars indicate events with uncertain flare classes, which have no observed flares. The arrows and numbers indicate the average values for flares with known flare classes. The average flare class of flares associated with the main CMEs of groups I and II is larger than that of the other two groups.

(A color version of this figure is available in the online journal.)

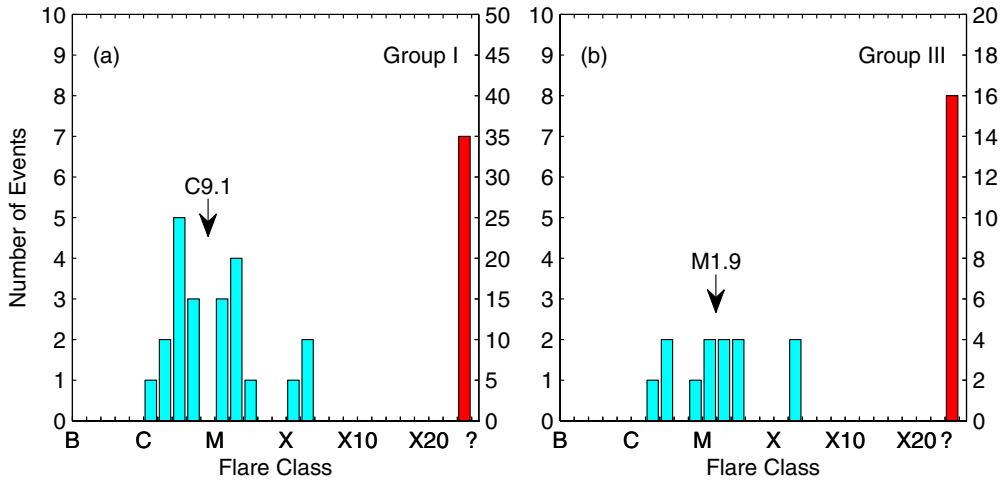

Figure 12. Similar to Figure 11, but for preceding CMEs of group I and group III.
(A color version of this figure is available in the online journal.)

CMEs because these CMEs have better magnetic connections to the Earth, then our findings can be summarized as (1) the likelihood of a "twin CME" leading to a large SEP event is 61% (43 out of 71); (2) the probability of a single fast CME leading to a large SEP events is 29% (16 out of 55); and (3) of all western large SEP events, 73% (43 out of 59) are caused by "twin CMEs."

Our findings suggest that the "twin-CME" scenario is a very likely scenario in generating large SEP events. Obviously it is not the only way of generating a large SEP event since 16 large SEP events do not agree with the "twin-CME" scenario. It is worth emphasizing that in the case of single fast CMEs, although no preceding CMEs existed, preceding flares were observed in many of those CMEs. For many such events, noticeable enhancements of particles at low-energy channels (*ACE*/ULEIS) and above 10 MeV nucleon^{-1} channels were observed. In these events, it is possible that some pre-acceleration occurred at the preceding flares, and they were later further accelerated at the shock driven by the fast CME. A possible reason that they did not lead to large SEP events is that the lack of a preceding CME prevents these pre-accelerated seed populations from being bound close to the CME-driven shocks that followed the flares.

Not all twin CMEs lead to large SEP events. Assuming the "twin-CME" scenario is indeed a very effective way to generate large SEP events, then one possible reason that these seemingly "twin-CME" events do not lead to large SEP events could be that they were mistakenly identified as twin CMEs. This is possible because while the preceding CME and the main CME can erupt from the same source region, they can propagate along different directions and the main CMEs may not go through the enhanced turbulence downstream of the first CME-driven shock. Since *SOHO*/LASCO can only provide a 2D view of a CME, it is possible that some of these "twin CMEs" are off-propagating twin CMEs and should not be classified as "twin CMEs." Furthermore, note that many of these events do show some enhancement at *ACE*/SIS energy channels. Perhaps the reason they failed to be large SEP events is because the underlying shock acceleration process in these events was not efficient enough. This is possible since besides seed populations, many other factors, including shock geometry and shock strength, etc., have been shown (Li et al. 2005, 2009, 2012b; Tylka et al. 2005; Giacalone 2005a, 2005b) to be also able to affect the particle acceleration process. Therefore, having "twin CMEs" does not guarantee a large SEP event.

Finally, in Section 2.3, we discussed that seven "twin-CME" events did not show enhancements at the *ACE*/ULEIS energies. Among these, the 1999 September 9, 1999 November 16, 2000 March 4, and 2002 May 22 events had no preceding flares and the 2002 March 20, 2002 November 11, and 2003 March 19 events had preceding flares. Since there were no enhancements in both *ACE*/ULEIS and *ACE*/SIS, there is the possibility that the magnetic connectivity to the Earth in these events was poor. Poor magnetic connectivity can be due to, e.g., coronal holes (Gopalswamy et al. 2009a, 2009b; Shen et al. 2006). Further detailed examination of these six events will help to better understand and constrain the "twin-CME" scenario.

We note that our studies only showed that the "twin-CME" is a possible scenario for large SEP events. There could be other possible ways to generate large SEP events. In particular, we note that preceding flares within 9 hr of the main CMEs can also pre-accelerate particles to provide the seed populations. Indeed, in group III many events have preceding flares as well as preceding CMEs, and in group IV, many events have preceding flares although no preceding CMEs existed. In both cases, in situ enhancement at *ACE*/ULEIS energies were found. For group III, it is difficult to discern the role of the preceding flares and that of the preceding CMEs. For group IV, the role of preceding flares is clear since no preceding CMEs existed. Compared to the "twin-CME" scenario, the preceding flares did not have a strong turbulence that existed downstream of the first CME which keeps the seed particle close to the Sun. This is perhaps the reason that group IV events were not intense enough to become large SEP events. Further studies of the role of preceding flares in large SEP events and non-large SEP events will be important to better understand the "twin-CME" scenario. However, such a study is beyond the scope of this paper.

Statistical analyses on the time intervals between the preceding CMEs and the main CMEs, on the CME widths, on the CME speeds, and on the associated flare classes have also been performed. The results are shown in Section 3.

In summary, we found that most large SEP events in solar cycle 23 are in agreement with the "twin-CME" scenario proposed by Li et al. (2012a). However, we do note that the generation of a large SEP event is a complicated process. In this paper we limit ourselves to discussing only the

"twin-CME" scenario as a possible scenario. We note that although the statistical study we presented in the previous section appears to be supportive of the "twin-CME" scenario, the "twin-CME" scenario is not the only scenario for generating a large SEP event.

From the point of view of space weather, our study suggests that single fast CMEs, while capable of interacting with Earth's magnetosphere and very geo-effective, more than 50% of the time do not lead to a large SEP event (see Figure 1). The resulting radiation dose from energetic particles can be within the tolerable limit. However, if preceding CMEs exist, even quite small ones, the chance of the main CME leading to a large SEP event will increase significantly. Since these preceding CMEs could be small, monitoring them is not easy. In particular, correctly identifying the propagation directions of the preceding CMEs and the main CMEs may be crucial in identifying a real "twin-CME" event. This issue will be investigated in a future work.

This work is supported in part by an Innovation Program Award for Graduate Student in Jiangsu (CXZZ11_0625) and Nanjing University of Information Science and Technology Excellent Teachers Scholarship for Overseas Studies for L.D. and NSF41174165 for Y.J., and NSF grants ATM-0847719, AGS1135432, AGS0962658, and NASA grant NNH07ZDA001N for G.L. and L.Z. at UAHuntsville. We thank the referee for valuable suggestions in producing Figures 2 and 3.

REFERENCES

Baker, D. N. (ed.) 2004, Space Weather: The Physics Behind a Slogan (Berlin: Springer), 656
Cane, H. V., McGuire, R. E., & von Rosenvinge, T. T. 1986, ApJ, 301, 448
Cane, H. V., Mewaldt, R. A., Cohen, C. M. S., & von Rosenvinge, T. T. 2006, JGR, 111, A6
Cane, H. V., Richardson, I. G., & von Rosenvinge, T. T. 2010, JGR, 115, A08101
Chen, C., Wang, Y., Shen, C., Ye, P., Zhang, J., & Wang, S. 2011, JGR, 116, A12108
Cohen, C. M. S., Mewaldt, R. A., Cummings, A. C., et al. 2003, AdSpR, 32, 2649
Cohen, C., Mewaldt, R., Leske, R., et al. 2007, SSRv, 130, 183
Desai, M. I., Mason, G. M., Dwyer, J. R., et al. 2003, ApJ, 588, 1149
Desai, M. I., Mason, G. M., Wiedenbeck, M. E., et al. 2004, ApJ, 611, 1156
Evans, R. M., & Opher, M. 2008, ApJ, 687, 1355
Giacalone, J. 2005a, ApJ, 628, L37
Giacalone, J. 2005b, ApJ, 624, 765
Gopalswamy, N., Mäkelä, P., Xie, H., Akiyama, S., & Yashiro, S. 2009a, JGR, 114, A00A22
Gopalswamy, N., Makela, P., Xie, H., Akiyama, S., Yashiro, S., et al. 2009b, in AIP Conf. Proc. 1216, Twelfth International Solar Wind Conference, ed. M. Maksimovic, K. Issautier, N. Meyer-Vernet, M. Moncuquet, & F. Pantellini (Melville, NY: AIP), 452
Gopalswamy, N., Xie, H., Yashiro, S., & Usoskin, I. 2010, IJRSP, 39, 240
Gopalswamy, N., Yashiro, S., Krucker, S., Stenborg, G., & Howard, R. A. 2004, JGR, 109, 602
Ho, G. C., Mason, G. M., Roelof, E. C., Gold, R. E., & Mazur, J. E. 2003, AdSpR, 32, 561
Kahler, S. W. 1982, JGR, 87, 3439
Kahler, S. W. 1996, in AIP Conf. Proc. 374, High Energy Solar Physics, ed. R. Ramaty, N. Mandzhavidze, & X.-M. Hua (Melville, NY: AIP), 61
Kahler, S. W. 2005, JGRA, 110, A12
Kahler, S. W., & Reames, D. V. 2003, ApJ, 584, 1063
Kahler, S. W., Reames, D. V., & Burkepile, J. T. 2000, in ASP Conf. Ser. 206, High Energy Solar Physics Workshop, ed. R. Ramaty & N. Mandzhavidze (San Francisco, CA: ASP), 468
Klecker, B., Möbius, E., Popecki, M., et al. 2009, Proc. 31st Int. Cosmic Ray Conf., Łódź, Poland, http://icrc2009.uni.lodz.pl/proc/pdf/icrc0278.pdf
Lanzerotti, L. J. 2001, GMS, 125, 11
Li, G., Moore, R., Mewaldt, R. A., Zhao, L., & Labrador, A. 2012a, SSRv, 171, 141
Li, G., Shalchi, A., Ao, X., Zank, G., & Verkhoglyadova, O. P. 2012b, AdSpR, 49, 1067
Li, G., Webb, G., Shalchi, A., & Zank, G. 2009, in AIP Conf. Proc. 1183, Shock Waves in Space and Astrophysical Environments, ed. A. Xianzhi, G. Zank, & R. Burrows (Melville, NY: AIP), 57
Li, G., & Zank, G. 2005, in AIP Conf. Proc., 781, The Physics of Collision Less Shocks, ed. Li Gang, G. P. Zank, & C. T. Russell (Melville, NY: AIP), 233
Li, G., Zank, G. P., & Rice, W. K. M. 2005, JGR, 110, 1
Mason, G. M., Mazur, J. E., & Dwyer, J. R. 1999, ApJL, 525, 133
Mason, G. M., Dwyer, J. R., & Mazur, J. E. 2000, ApJ, 545, L157
Mason, G. M., Mazur, J. E., & Dwyer, J. R. 2002, ApJ, 565, L51
Mason, G. M., Desai, M. I., Mazur, J. E., & Dwyer, J. R. 2005, in AIP Conf. Proc. 781, The Physics of Collisionless Shocks, ed. Li Gang, G. P. Zank, & C. T. Russell (Melville, NY: AIP), 219
Mertens, C. J., Kress, B. T., Wiltberger, M., et al. 2010, SpWea, 8, S03006
Mewaldt, R. A., Cohen, C. M. S., Labrador, A. W., et al. 2005, JGR, 110, 038
Mewaldt, R., Cohen, C., Mason, G. M., et al. 2007, SSRv, 130, 207
Olmedo, O., Zhang, J., Wechsler, H., Poland, A., & Borne, K. 2008, SoPh, 248, 485
Reames, D. V. 1995, AdSpR, 15, 41
Reames, D. V. 1999, SSRv, 90, 413
Shen, C., Wang, Y., Ye, P., & Wang, S. 2006, ApJ, 639, 510
Siscoe, G. 2000, JATP, 62, 1223
Tylka, A. J., Boberg, P. R., Adams, J. H., et al. 1995, ApJ, 444, L109
Tylka, A. J., Cohen, C. M. S., Dietrich, W. F., et al. 2005, ApJ, 625, 474